

**Experimental Development of Improved Vehicle
Compatibility – Final Report**

by
Dr H C Davies

PPR134

PUBLISHED PROJECT REPORT

TRL Limited



PUBLISHED PROJECT REPORT PPR134

**EXPERIMENTAL DEVELOPMENT OF IMPROVED VEHICLE
COMPATIBILITY - FINAL REPORT**

Version: Final

by Dr H C Davies (TRL Limited)

Prepared for: Project Record: Development of Improved Vehicle Compatibility
Client: Dr R M Kimber (Science and Engineering Director -
Transport Research Foundation)

Copyright TRF Limited July 2006

This report has been prepared for the Transport Research Foundation. The views expressed are those of the author(s) and not necessarily those of the Transport Research foundation.

Approvals	
Project Manager	Dr Huw Davies
Quality Reviewed	Dr Mervyn Edwards

This report has been produced by TRL Limited, under/as part of a Contract placed by the Transport Research Foundation. Any views expressed are not necessarily those of the Transport Research Foundation.

TRL is committed to optimising energy efficiency, reducing waste and promoting recycling and re-use. In support of these environmental goals, this report has been printed on recycled paper, comprising 100% post-consumer waste, manufactured using a TCF (totally chlorine free) process.

CONTENTS

Executive summary	i
1 Introduction	1
2 Compatibility Performance Assessment Approach	1
2.1 Full width deformable barrier (FWDB) test for structural interaction	2
2.2 Offset deformable barrier (ODB) test at 64km/h for frontal force matching	3
2.3 Offset deformable barrier (ODB) test at 80km/h for compartment strength	4
2.4 Frontal offset car-to-car impact test for barrier test validation	4
3 Assessment of Test Car Compatibility Performance	5
3.1 Test car front structure	5
3.2 Full width deformable barrier (FWDB) test	6
3.3 Offset deformable barrier (ODB) test at 64km/h	11
3.4 Assessment summary and recommendations for improvement	13
4 Improvement of Test Car Compatibility Performance	14
4.1 Test car modification	14
4.2 Compatibility performance assessment – FWDB test	18
4.3 Improvement of test car compatibility performance summary	25
5 Concept Modelling Technique Development	27
5.1 Development of the methodology	28
5.2 Validation of the methodology	30
5.3 Concept model development summary	32
6 Conclusions	32
7 References	34

Executive summary

Addressing vehicle crash compatibility is now recognised as the next major step forward in the improvement of car occupant secondary safety. The research reported here was undertaken as part of a Transport Research Foundation (TRF) funded programme aimed at defining innovative approaches to improve car compatibility performance. Two different research activities are discussed, the first focused on assessment and improvement of existing car compatibility performance, the second on development of a concept modelling technique to investigate compatibility performance at the concept design stage.

A proposed method of assessing vehicle compatibility performance focuses on a suite of three car-to-barrier tests, each test measuring one aspect of the compatibility performance: structural interaction, front force level matching and compartment strength. The approach to assessing car compatibility performance defined as part of this research builds upon that method by detailing a number of additional analyses that would help us understand and identify the reasons for a particular car's measured compatibility performance. The outcome is a methodology that provides both compatibility performance assessment and recommendations for improved crash compatibility.

This methodology was applied to a test car already considered to demonstrate many of the principles behind improved compatibility: multiple load paths and good shear connections. In order to confirm the validity of the recommendations, the research then undertook modifications to the test car of the 'add-on' type focused on improvement in structural interaction potential because structural interaction is viewed as a prerequisite for improved compatibility. The structural interaction compatibility performance of the modified car was then assessed using the appropriate car-to-barrier test (full width deformable barrier test) and compared to that of the unmodified test car.

It was found that the modifications were successful in improving the front force distribution of the car structure. The frontal force distribution is acknowledged as a basis for measurement of structural interaction potential. However, improvements in the assessment metric measures were only marginal for the modified car due to alteration in force distribution ahead of the principal load paths. It should be noted that the area for the homogeneity assessment had to be reduced due to the low frontal height of the test car. This emphasises the need for an assessment area definition based on car geometry or a fixed area that all cars can be expected to load. It was considered that further modifications to the existing car structure beyond 'add-on' modifications would further improve the force distribution although these were not investigated.

For initial concept design type studies, mathematical models are required that are simple to alter and computationally inexpensive. Full scale Finite Element (FE) models are not ideally suited to this as they have large CPU requirements and alterations to the model can sometimes be time consuming. Simple FE models that use beam elements to represent a car's main structures are suitable for this type of work. However, to be able to use them, an efficient way to estimate the beam element properties is required. A tool to estimate the beam element properties of a section and translate them into a format suitable for input into the material model in a LS-DYNA input deck has been developed as part of this research. This can also be used to estimate possible section sizes for given axial crush and bending moment requirements. However, it should be noted that the methodology on which this is based has only been validated for a limited range of section sizes and shapes, i.e. simple thin walled rectangular and square sections with a t/b ratio between 0.007 and 0.02, where t is the thickness and b the width of the buckling (largest) plate.

1 Introduction

In the UK, over half of the deaths and serious injuries to car occupants in road accidents occur when one car collides with another (Edwards et al, 2001). Research into crash compatibility aims to minimise overall injury severity in such collisions by encouraging the car structures to work together better. It is now widely believed that improving compatibility is the next major step in the improvement of car occupant secondary safety.

To date, compatibility research has focused on frontal impact collisions as this is where the greatest potential benefits can be achieved (Edwards et al, 2000). This research has led to an understanding of current compatibility problems and proposals for test procedures to assess and control compatibility (O'Reilly 2001; Diboine et al, 2002; Edwards et al, 2003). However, little work has been published on more compatible car designs, apart from a few exceptions such as Honda's ACE^{TM*} concept design.

As part of ongoing Department for Transport (DfT) sponsored research into compatibility being undertaken by TRL, a current European mid-sized car was modified to improve its compatibility (Edwards et al, 2003). However, these modifications were introduced only with the aim of demonstrating the principles behind improved crash compatibility and severely compromised the existing functionality of the car. Further to this research a separate programme funded by the Transport Research Foundation (TRF) was initiated. The aim was to define an innovative approach to the investigation of car compatibility performance that would, in addition to measuring car compatibility performance, result in recommendations to improve upon that performance without placing unreasonable limitations on existing vehicle functionality.

Described here is an approach to assess car compatibility performance in frontal impact based upon three car-to-barrier test procedures. The experimental application to a test car aimed to provide both a compatibility performance measure and recommendations for improvement. Based upon the subsequent recommendations, modifications were made to the test vehicle aimed at improving the structural interaction aspect of compatibility performance. An assessment was then made of how well the modifications had improved the car's compatibility performance. Also described is the development of a tool to calculate a section's beam element properties for input into concept type FE models. Such models are ideally suited to studies at the 'concept development' stage of a vehicle's design, as they can be changed quickly and easily and require little computer processing time, so that many simulations can be performed and allow for the structural integration of cars to be investigated at the concept design stage.

2 Compatibility Performance Assessment Approach

Research studies for frontal impact have shown that for compatibility, cars need to interact in a predictable manner to absorb the impact energy with minimal occupant compartment intrusion over a broad range of collision types. In order to achieve this, an essential prerequisite is good structural interaction. Current vehicle front structures predominantly consist of fore/aft structural members with a combined frontal area far lower than that of the actual vehicle. It is the misalignment of these structural members in car-to-car collisions that lead to problems of under/overriding and lateral fork effect, which limit the energy absorption of the vehicle frontal structure and result in occupant compartment intrusion at lower than expected impact severities. Some form of frontal force matching will also be necessary to ensure that the impact energy is absorbed without exceeding the strength of the occupant compartment. For good structural interaction, the requirement is for multiple load paths with strong lateral and vertical shear connections, in particular at the front of the car, to ensure engagement of the opposing car structures and that the impact loads are directed into the principal energy absorbing components. For frontal force matching, the requirement is for the car frontal structure to be capable of absorbing its own impact energy without exceeding a certain force level, which has still to be determined. The compartment strength would then have to be strong enough to withstand this maximum frontal force level.

* ACETM – Advanced Compatibility Engineering

To assess and control crash compatibility a suite of three test procedures has been proposed (Edwards et al, 2003). These are:

- Full width deformable barrier (FWDB) impact at 56km/h for structural interaction.
- Offset deformable barrier (ODB) impact at 64km/h for frontal force matching.
- Offset deformable barrier (ODB) impact at 80km/h for compartment strength.

The full width and offset deformable barrier impact test configurations are shown in Figure 1 and Figure 2 respectively.

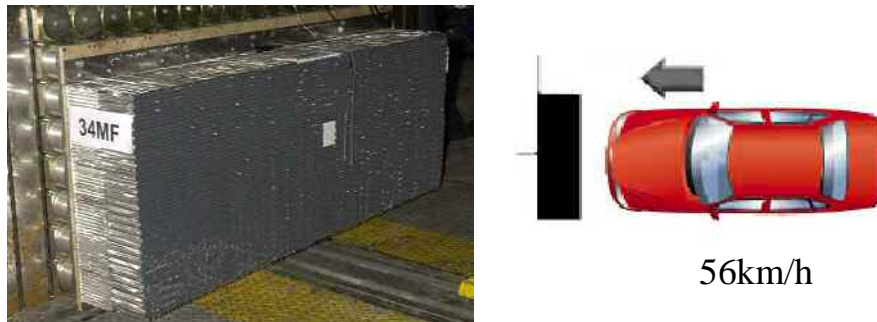


Figure 1: Full width deformable barrier test configuration.

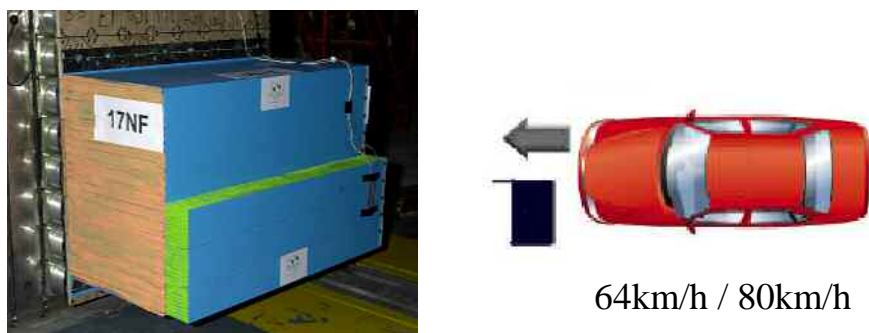


Figure 2: Offset deformable barrier test configuration.

It should be noted that two of the three proposed tests are adaptations of current self-protection assessment tests, so only one additional test is proposed for compatibility. The FWDB and 64km/h ODB tests are modifications of the US NCAP* and EuroNCAP† frontal impact tests respectively.

The definition of an approach to assess car compatibility performance based on the three test procedures is described below. Because these test procedures have not yet been completely validated, the approach contains additional car-to-car tests that if necessary can be used to confirm the findings of the barrier test.

2.1 Full width deformable barrier (FWDB) test for structural interaction

The purpose of this test is to assess structural interaction potential using a measurement of the car frontal force distribution measured on a high-resolution load cell wall (LCW) behind the deformable face. The premise is that cars with a more homogeneous frontal force distribution should offer greater potential for good structural interaction with other cars. The purpose of the deformable barrier and the development of a metric for the assessment of the homogeneity of the force distribution have been described previously (Edwards et al, 2003). Further details of the test setup and the ‘homogeneity criterion’ metric are available in a test protocol (VC-Compat, 2003). Since the issue of that document,

* US NCAP – United States New Car Assessment Programme

† EuroNCAP – European New Car Assessment Programme

a revised homogeneity metric, referred to as the ‘relative homogeneity criterion’, has been developed to overcome a mass dependency problem.

The following steps are recommended to assess a car’s structural interaction potential using the FWBD test results:

- Firstly, the Average Height of Force (AHOF) (Summers et al, 2002), relative homogeneity criterion and the LCW peak force are calculated. These measures are used to compare the compatibility performance of the car with other cars tested. The AHOF gives an indication of whether the height of the car’s main structure is in alignment with that of other cars. The vertical and horizontal components of the relative homogeneity criterion give an initial indication of the car’s susceptibility to under/override* and lateral fork effect†, respectively. The LCW peak force is used to provide an indication of the frontal force levels of the car in this impact configuration.
- Following this, a more detailed assessment of the LCW force distribution is made focusing on the force time history recorded by each load cell. In the vertical direction, an assessment of the number of load path levels, their relative distribution and strength is made. In the horizontal direction the effectiveness of lateral connections, such as the bumper beam, are determined. Structures that impact more than one load cell require that the force time histories from the impacted cells are grouped in order to determine the peak load. The barrier deformation is also examined to further understand how the car structure loads the wall. This understanding is required to determine, for example, if a car’s lower rails and bumper beam loaded one or two rows of load cells, as this can potentially alter the relative homogeneity measure significantly. To further understand issues such as the contribution of power train deceleration loads to the LCW force and distribution, the deceleration of the car’s constituent components is examined.
- Finally, the car deformation is examined to assess how the structure performed. From this it is assessed how the activated load paths functioned, if any components failed or were close to failure and the stability of the frontal structure.
- In addition, for good compatibility a car must also have an adequate level of self-protection. To ensure that this is the case, the dummy injury criteria and occupant compartment stability are assessed based on appropriate legislative and consumer testing protocol. It should be noted that this test configuration generates a high occupant compartment deceleration pulse that is especially demanding of the restraint system.

2.2 Offset deformable barrier (ODB) test at 64km/h for frontal force matching

The purpose of this test is to assess the car frontal force level by measuring the peak load applied to a load cell wall (LCW) behind the deformable barrier face. Limiting the frontal force level by limiting the peak load, together with a strong compartment, will allow for each vehicle to absorb its share of the impact energy within the front structure without significant compartment intrusion. Details and a demonstration of this approach have been reported previously (Edwards et al, 2000; 2001). As part of the compatibility performance assessment, additional instrumentation consisting of accelerometers mounted to component parts of the car and structure are used.

The following steps are recommended to assess the car’s frontal force level using the 64km/h ODB test results:

- The peak load cell wall force is used as a measure of the frontal force level. As a performance requirement for the maximum acceptable force level has still to be determined, a comparison is made with the peak force level from other vehicles tested, in particular those vehicles of a similar mass, to ascertain how similar it is.

* Under/override – Vertical misalignment of the load bearing structure during the impact.

† Fork Effect – Lateral misalignment of the load bearing structure during the impact.

-
- The decelerations of the constituent parts of the car are used to determine the contribution to the load cell wall force of the deceleration of the occupant compartment and the deceleration of the mainly rigid masses forward of the firewall. This can be used to check the minimum strength of the occupant compartment in this test configuration and whether the engine bottomed out on the load cell wall towards the end of the impact.
 - In addition, the frontal force distribution and the deformation of the vehicle and the barrier face are analysed to give some indication of the structural interaction performance of the vehicle in this test and confirm observations from the FWDB test assessment. How the activated load paths functioned, if any components failed or were close to failure and the stability of the frontal structure is assessed. The LCW force distribution is used to detect aggressive features. The deformation of the car and barrier is used to assess the performance of frontal lateral and vertical connections. It should be noted that a high-resolution LCW measurement is required for this analysis.
 - In addition, for good compatibility a car must also have good self-protection. This test configuration provides a severe deformation to one side of the car that can be used to assess the occupant compartment integrity and the performance of the restraint system based on appropriate legislative and consumer testing protocol.

2.3 Offset deformable barrier (ODB) test at 80km/h for compartment strength

The 64km/h offset deformable barrier test, if the occupant compartment remains stable, will only provide information about the car's ability to cope with peak loads up to that generated by the car itself. It is necessary to be able to show that an occupant compartment can survive the forces imposed by another car, which may generate a higher frontal force but be within any future front force level requirements. An offset test at an increased speed of 80km/h can provide important information concerning the strength of the occupant cabin. This test is similar to that of the 64 km/h test except that the dummies are uninstrumented as there is no requirement that cars provide a survivable performance for the occupants at this impact severity – it is a measure of the compartment strength only. A load cell wall is used to record the compartment strength whilst accelerometers attached to the car structure provide important information concerning the collapse mechanism of the occupant compartment.

The following steps are recommended for the assessment of the occupant compartment strength using the 80km/h test results:

- At the end of the impact the engine has bottomed out the deformable barrier face and stopped decelerating. The load cell wall force at this point consists mainly of the occupant compartment force component and represents the load imposed on the compartment and hence can be used as an indication of the minimum load that the compartment can withstand for this impact configuration.
- If the compartment becomes unstable during the impact, it is necessary to ensure that the strength measured is prior to any major intrusion occurring. Assessment of the compartment deformation is used to determine whether the compartment became unstable during the impact

2.4 Frontal offset car-to-car impact test for barrier test validation

The three car-to-barrier tests described should be sufficient to provide an assessment of a car's compatibility potential. However, because these test procedures have not yet been completely validated, additional car-to-car tests may be needed to confirm the findings of the car-to-barrier tests. It is recommended that these tests should be performed with a closing speed of 112 km/h and an offset of 50 percent; overlap measured from the narrower of the two test vehicles. This is because, if only a single test can be chosen, this configuration is the most representative of the majority of severe injury accidents (Delannoy et al, 2003). Also the 64km/h ODB test is representative of this accident

configuration; a car's Energy Equivalent Speed (EES) in the car-to-car test configuration described approximately the same as in a 64 km/h ODB test. The EES is the speed at which the car has an energy equivalent to that absorbed by the car in the impact test.

In general, manufacturers aim to design their cars to perform well and predictably in a 64km/h ODB test, so the performance of a car in this test can be used as a benchmark. Therefore, one way to judge the compatibility performance of the cars in the car-to-car test is to compare their relative performances in this test and 64km/h ODB tests. If they have performed in a predictable compatible manner, with each vehicle absorbing its own share of the kinetic energy, then each car's performance will be similar to its performance in the 64 km/h ODB test. In contrast, if the cars did not behave in a compatible manner, at least one car's performance will be significantly worse than in the 64km/h ODB test.

What cars are chosen for this test depends on what aspect of compatibility the engineer wishes to confirm or investigate further. For example, for aspects of structural interaction, a car-to-car test using identical cars would normally be recommended as this minimises the effect of vehicle stiffness. If over/underride was of particular concern a test series altering the ride height of the cars could be performed to investigate in further detail.

3 Assessment of Test Car Compatibility Performance

Assessment of the test car's compatibility performance was based on FWDB and 64km/h ODB impacts test results. The 80km/h ODB test was not performed due to limited funding.

3.1 Test car front structure

The front structure of the test car consists of three levels of fore/aft load paths, these being in order from the ground level up the subframe rails, lower rails and upper rails (Figure 3). Connecting these load paths across the front of the car are a number of lateral (Figure 4) and vertical (Figure 5) shear connections

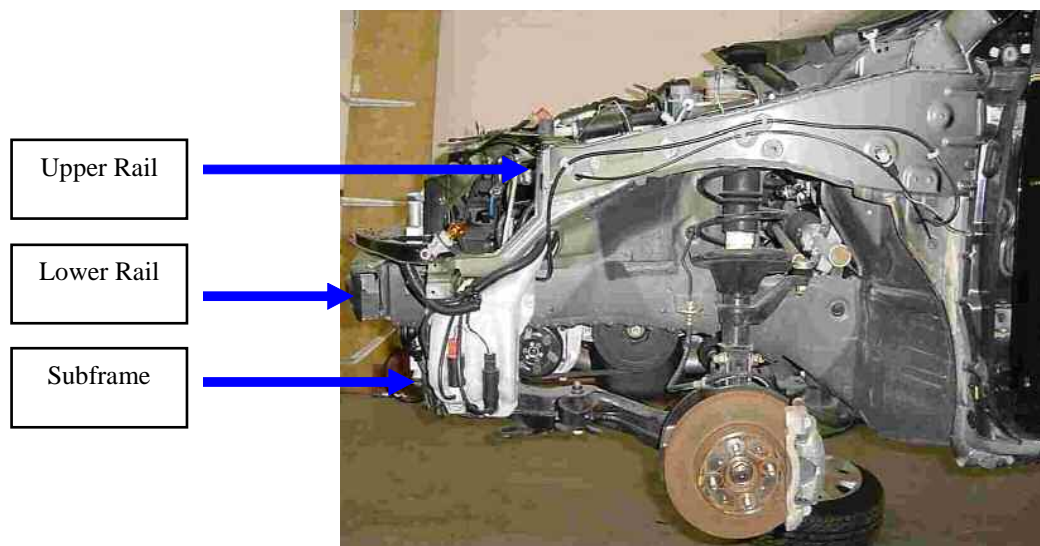


Figure 3: Side view showing the three identifiable levels of load paths.

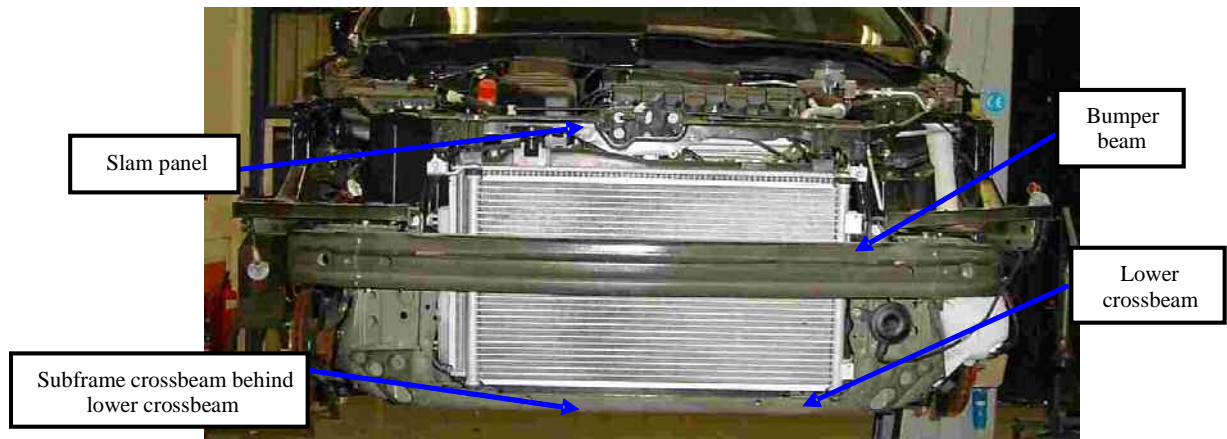


Figure 4: Front of car showing lateral connecting beams.



Figure 5: Side view of car showing front vertical shear connections.

3.2 Full width deformable barrier (FWDB) impact

The load cell wall force distribution for the test car is shown together with the outline of the main structural members (Figure 6). The high loads in E5:E7 and L5:L7 were generated by the impact of the lower rails, subframe rails and the vertical connections between these rails.

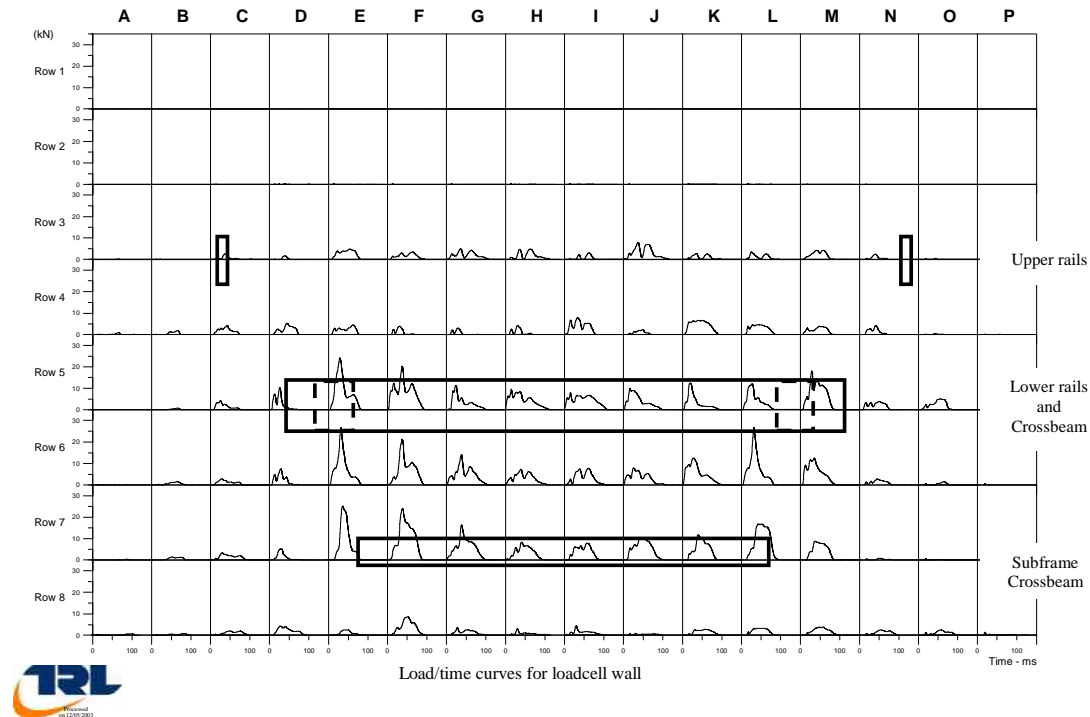


Figure 6: Force against time plot for all load cells showing the pre-impact alignment of the principal structural members.

The average height of force measurement for the unmodified test car was calculated as 391mm taking into account that the dynamic ride height of the car was 4mm higher than its static ride height. This AHOF measure is slightly below the bumper beam zone defined in FMVSS* part 581 that is generally used for the purpose of car front structure height comparison; FMVSS part 581 bumper beam zone is from 406mm to 508mm.

The relative homogeneity criterion was calculated for an assessment area (C3:N7)†. This is 12 columns wide and 5 rows high. The relative homogeneity criterion is compared with other cars that have been investigated at TRL (Figure 7); the lower the relative homogeneity criterion value the more homogeneous the frontal force distribution. It can be observed that the car generates a less homogeneous frontal force distribution than the other cars within the same class, although comparable with those cars in the family class and the single small SUV. Detailed examination of the load cell wall force distribution showed that the high vertical homogeneity value was due to the relative difference in the load applied by the three load path levels, particularly the low load applied by the upper load path level. The high value in the horizontal direction was caused by the low loading applied by the lateral front cross connections compared to that applied by the lower rail and subframe load paths. It was also noted that the alignment of the vehicle resulted in the crossbeam and lower rails bridging two rows of load cells.

* FMVSS – Federal Motor Vehicle Safety Standards

† The assessment area is a rectangle with load cell C7 (column; row) at the top left and N7 at the bottom right

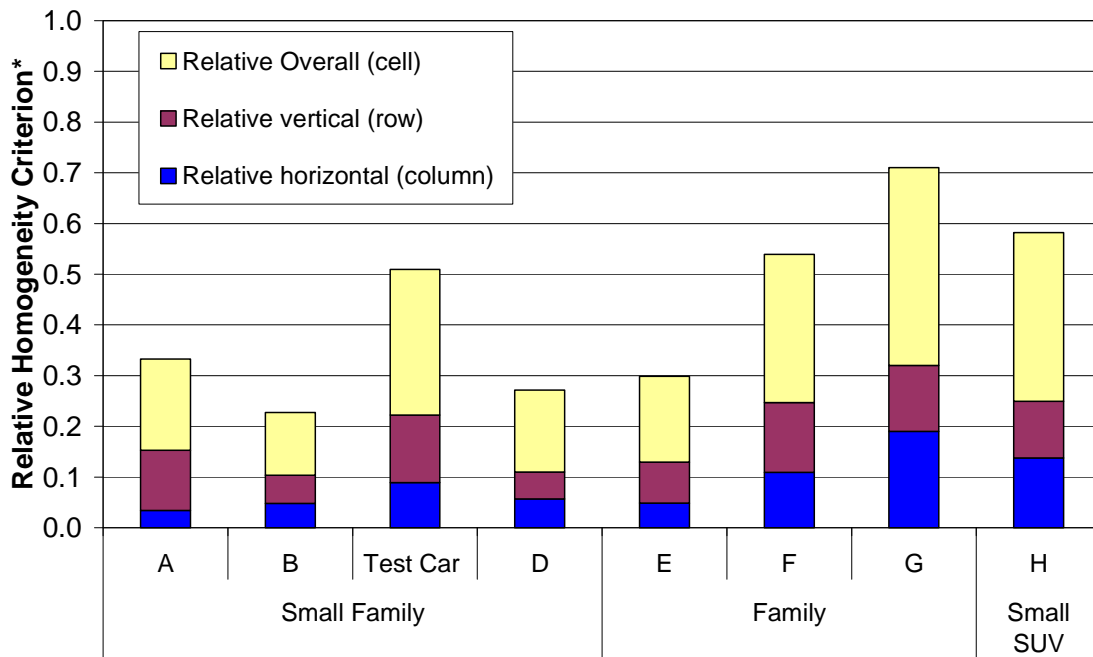


Figure 7: Comparison of unmodified test car homogeneity assessment with previously investigated cars based on a fixed assessment area being used (C3:N7). *Note that the lower the score, the better the homogeneity assessment and that the cars are ranked in mass order.

Examination of the deformed car structure showed both the lower rail and the subframe load paths failed in bending; the lower rails about the vertical axis and the subframe rails about the horizontal axis (Figure 8 and Figure 9). The failure of the subframe load paths and the RHS lower rail occurred at a narrowing of the beam cross section whilst the failure of the LHS lower rail occurred at a discontinuity caused by the attachment of an engine mounting to the upper surface.

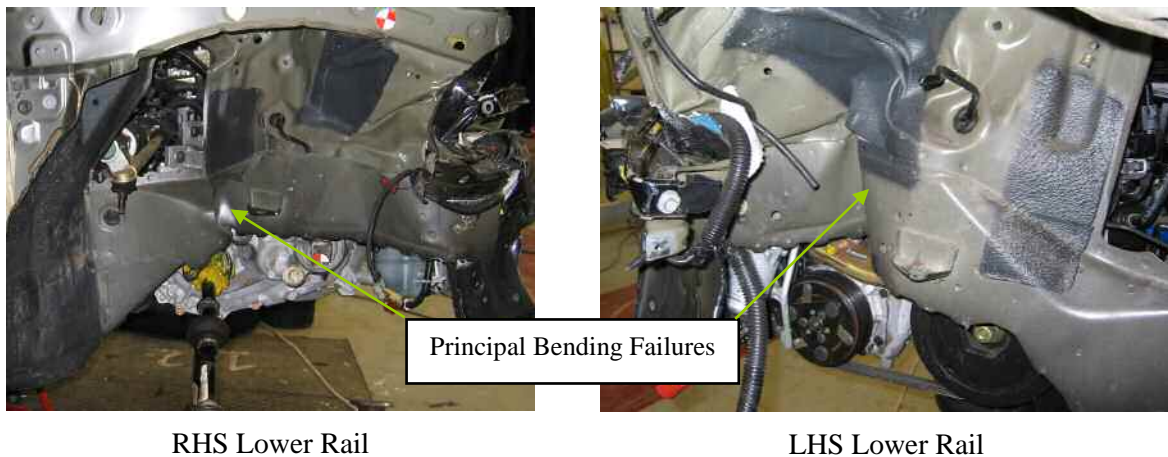


Figure 8: Lower rail deformation showing the principal failures in bending about the vertical axis.

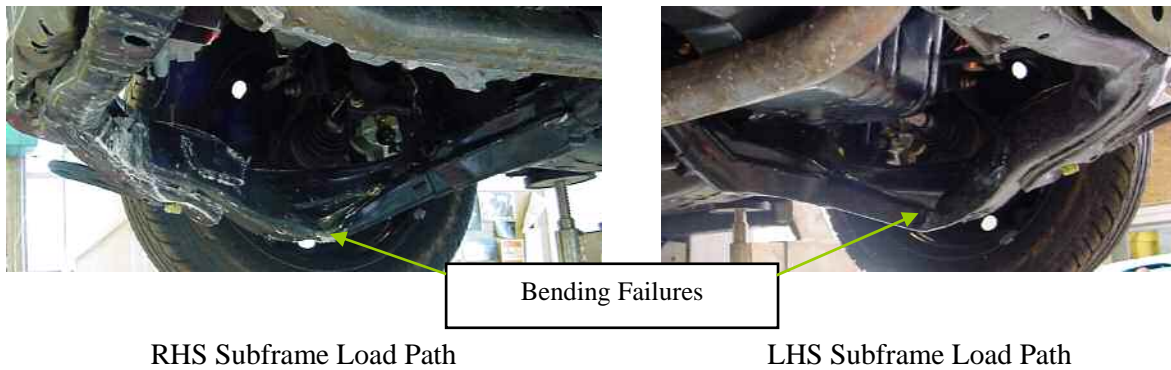


Figure 9: Subframe load path deformation showing the failures in bending about the horizontal axis.

The upper rails were determined to have been set too far back relative to the car leading edge to directly load the stiffer rear layer of the barrier face and therefore apply any significant load to the load cell wall. The RHS upper rail exhibited only minor distortion due to interaction with the softer front layer of the barrier face, whilst the LHS upper rail had failed in bending due to distortion of the shear connection with the lower rail (Figure 10).

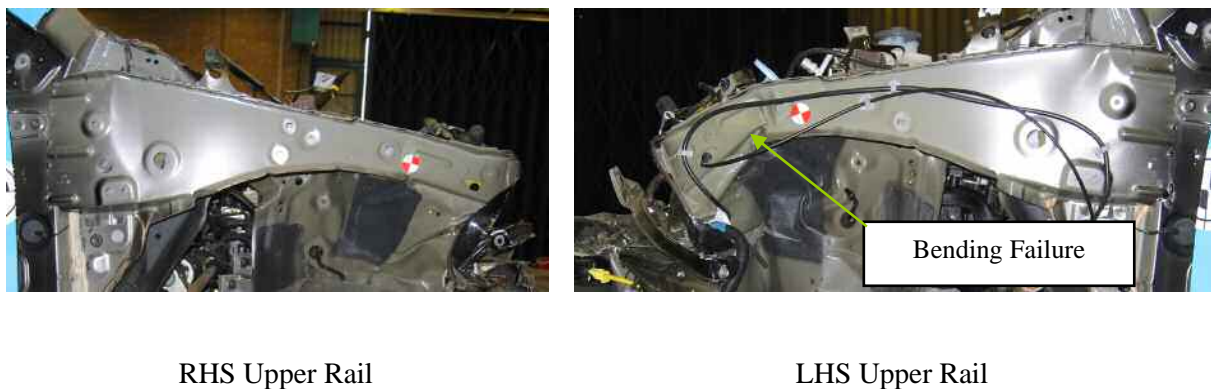


Figure 10: Upper Rail deformation showing no failure for the RHS upper rail and the failure in bending of the LHS upper rail.

Regarding the lateral shear connections, both the slam panel and the bumper crossbeam were observed to have failed in bending with the centre section displaced rearwards relative to the load path leading edge (Figure 11 and Figure 12). The slam panel failed through contact with the softer front layer of the deformable barrier element indicating the low shear strength of this beam whilst the bumper beam failed through contact with the stiffer rear layer. Both the bumper beam and slam panel remained attached to the leading edge of the lower rails and subframe load paths respectively. In addition, it was noted that the vertical shear connections between the lower rails and subframe were still connected post impact and showed no signs of failure.

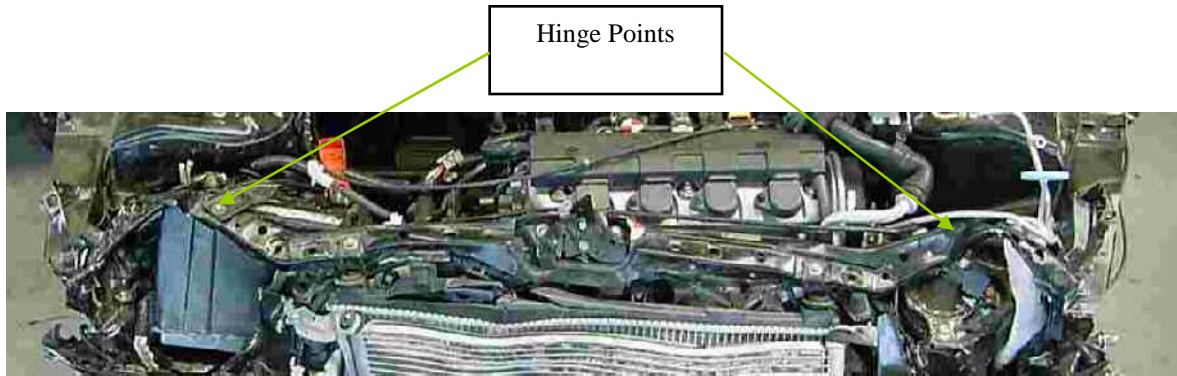


Figure 11: Slam panel deformation showing the location of the hinge points allowing rearward translation relative to the upper rail leading edge due to loading by the barrier face.



Figure 12: Bumper beam post impact showing the location of the hinge points allowing rearward translation relative to the lower rail leading edge due to loading by the barrier face.

In terms of the self-protection, all the dummy injury criteria were below ECE Regulation 94 injury limits for front impact protection (Figure 13). However, there was a potential concern regarding the contact of the driver's chest with the steering wheel; chest compression ~90% ECE Regulation 94 limit. This may require retiming of the restraint system.

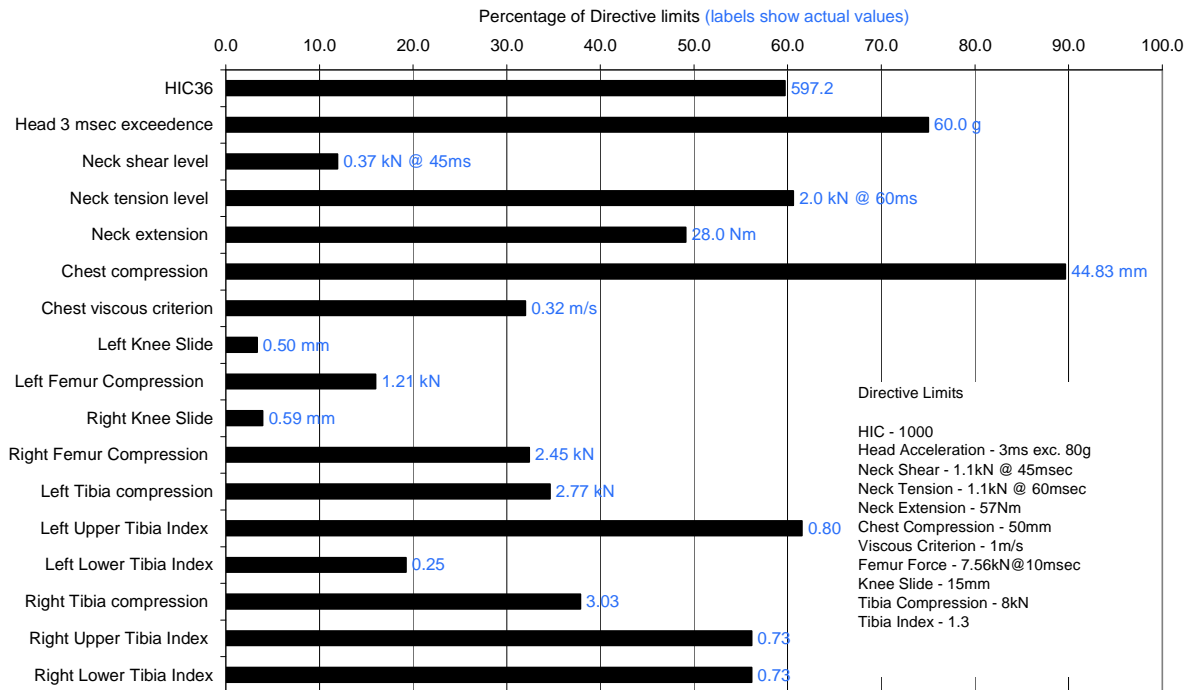


Figure 13: Driver dummy injury criteria expressed as a percentage of the ECE Regulation 94 limits.

3.3 Offset deformable barrier (ODB) test at 64km/h

In the offset test the peak load cell wall force was 410kN, the structural component was 310kN. The majority of this force was applied by the impacted side lower rail and to a lesser extent the subframe load path. Although it has yet to be determined what level the maximum frontal force level should be set in order to encourage compatibility, the peak force recorded by the test car is comparable to those cars within the same class that have been tested as part of EuroNCAP (Figure 14).

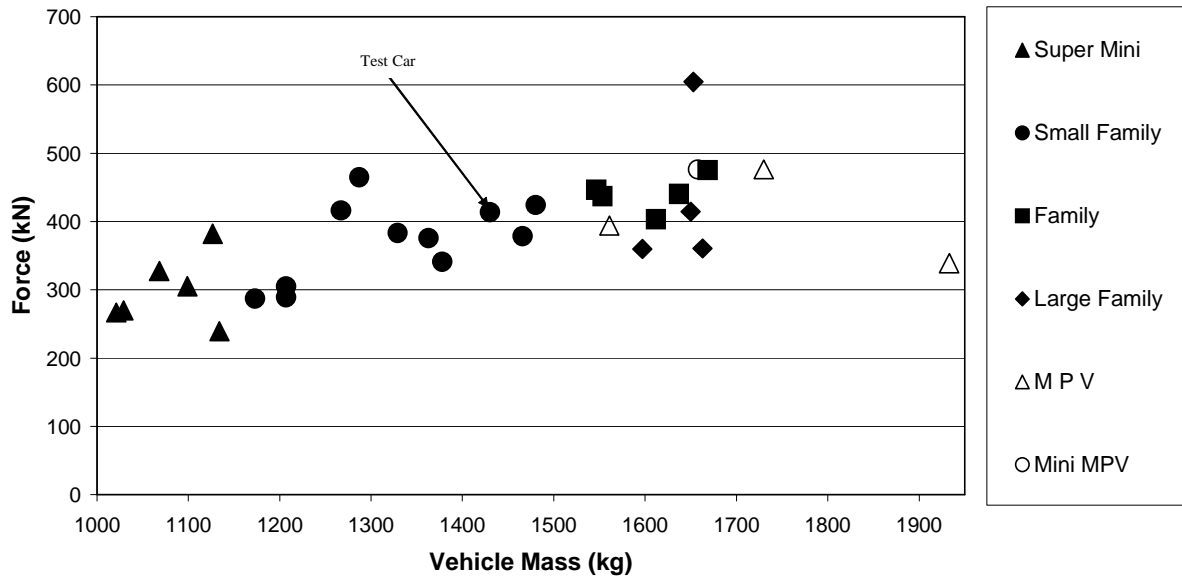


Figure 14: Comparison of the peak load cell wall force for the test car with other cars tested for EuroNCAP.

The deformation of the car front and barrier face indicated no potentially aggressive structures (Figure 15 and Figure 16). The slam panel was displaced rearwards relative to the leading edge of the car structure through contact with the deformable element, the performance of the slam panel in this test configuration confirming the earlier observation from the full width test regarding the low shear strength of this connection. In addition, it was noted that the front wheel on the impacted side had been displaced rearwards and came into contact with the sill forming an additional load path between the barrier face and the occupant compartment.



Figure 15: Post test driver's side and front view of the test vehicle.



Figure 16: Resultant deformable barrier face deformation showing the approximate impact locations of the main structural load paths.

In terms of the self-protection, the compartment remained stable based on EuroNCAP protocol and the dummy injury criteria were all below the ECE Regulation 94 injury limits for frontal impact protection.

3.4 Assessment summary and recommendations for improvement

Based upon the performance of the test car in FWDB and 64km/h ODB test configurations the following conclusions and recommendations were made regarding its compatibility performance:

- For the assessment area considered, the relative homogeneity criterion was higher (i.e. poorer) than for other cars within the same class, even though there was a good balance between the loads applied by the lower rail and subframe load paths. To improve homogeneity in the vertical direction, the load applied by the upper load path level should be increased by bringing structure further forward toward the leading edge of the car and increasing its crush strength. This would help reduce the potential for the car to be overridden in an impact with a car that has a higher frontal structure. The low load contribution from the upper load path level was also indicated the comparatively low AHOF assessment measure. To improve homogeneity in the horizontal direction, the shear strength of the bumper crossbeam and slam panel should be increased. This would help prevent the lateral fork effect in collision with other cars. In addition, increasing the frontal area of the subframe crossbeam would create a larger pushing surface which would benefit in engaging other car structures and provide a more homogeneous frontal force distribution on the load cell wall. However, the effects of additional structure forwards of the front axle on ride and handling must also be considered.
- There was good stability of the structure in the vertical direction, the lower rails failing in bending about the vertical axis minimising movement of the structure in the vertical direction during the impact.
- The frontal force level of the test car in the offset test was 410kN. Although no maximum acceptable force level has yet been specified for this test, this was comparable to other cars of a similar mass tested at TRL indicating that any structural modifications should aim to limit the overall increase in the frontal force level in this test configuration. The occupant compartment remained stable and the minimum compartment strength in this loading configuration was determined as 310kN.
- The lower vertical shear connection was effective in deforming the offset impact barrier. However, the upper vertical shear connection was a single panel and was not able to interact effectively with the barrier face. The frontal area of the upper shear connection would ideally

need to be increased to promote better interaction with the lateral crossbeams of another car that may lie between the height of the lower and upper load path levels of the test car.

- Regarding the self-protection, the dummy injury criteria in both the full width and offset impact test configuration were below the ECE Regulation 94 injury limits and the compartment remained stable based on EuroNCAP protocol. However, there was a possible concern regarding the contact of the driver's chest with the steering wheel in the full width impact test, which may require retiming of the restraint system.

4 Improvement of Test Car Compatibility Performance

It is the intention of the compatibility performance assessment detailed previously that modifications to the vehicle based on the resulting recommendations will improve the compatibility performance of the test car. To demonstrate this, the programme of research undertook modifications to the test car of the 'add-on' type based upon those recommendations aimed specifically at improving structural interaction potential. The structural interaction compatibility performance of the modified car was then assessed in comparison to the unmodified test car using the full width deformable barrier test.

The structural modifications were incorporated into the existing vehicle so that they had minimal effect upon the existing vehicle functionality; one of the principal considerations of this research. Mention is also made of the effect the modifications would have upon self-protection in a high deceleration test and where applicable the possible effect upon vehicle performance in the offset impact test configuration. A detailed assessment using the 64km/h ODD, 80km/h ODB and possibly car-to-car testing would be required to assess the effect of the modifications upon other aspects of the vehicle performance.

Described here are the modifications made to the test car and the assessment of its structural interaction compatibility performance using the FWDB test.

4.1 Test car modification

The upper load path level, comprising the upper rails and slam panel connection, was modified to increase load contribution and achieve a more homogeneous frontal force distribution. There was no alteration of the existing upper rails as in the previous full width test they were observed to be too far back to interact effectively with the deformable barrier face in this impact configuration and the vehicle outer profile at this level precluded extending the upper rails forward. The approach taken was to integrate into the existing vehicle structure additional upper rails slightly inboard of the existing rails and connecting to a revised slam panel (detailed later) at their leading edge and supported at the rear by the front face of the suspension housings (Figure 17). The cross section of these additional upper rails was maximised given existing vehicle packaging requirements and the centre line kept as close to that of the vehicle centreline as possible to encourage failure in axial crush. The only alteration required to the existing vehicle to accommodate these additional upper rails would be the rerouting of the air conditioning pipes from the LHS inner wing and the relocation of the battery on the RHS. Failure load of the additional upper rail structure was set at 20kN based upon estimate of the load that could be taken by the supporting structure; this is approximately 1/3rd that of the lower rail failure load measured in the previous full width impact test. Consideration should also be given to the possible negative effects in side impact of increasing crush strength of the upper load path and moving the leading edge forward. Further investigation of side impact compatibility is required.



Figure 17: Additional upper rail load paths connecting at the leading edge to the centre section of the revised slam panel and at the rear edge to the front face of the suspension turrets.

Improved load distribution in the lateral direction at this level was accommodated for by increasing both bending strength and frontal area of the centre section of the slam panel: that part supported by the additional upper rails (Figure 18). Part of this increase in bending strength was due to the greater cross-sectional depth in the fore/aft direction achieved by extending the beam rearwards into the engine bay. To minimise mass increase, holes were drilled in the upper and lower face of this beam.



Figure 18: Revised centre section of the slam panel crossbeam connecting the leading edges of the additional upper rails across the vehicle front.

For the principal load path level, consisting of the lower rails and bumper crossbeam, modifications focused on increasing the lateral load distribution. In the test with the unmodified car, the bumper crossbeam failed in plastic bending at either end due to loading from the barrier face. The centre section of the bumper beam was then translated rearwards relative to the lower rail leading edge with minimal additional loading. The approach taken was to increase the bending strength of the bumper beam. The existing cross-section of this beam was open at the rear. Therefore, to increase the bending strength and allow for additional compressive loading a closing panel was introduced (Figure 19).



Figure 19: Front crossbeam closing panel welded onto the existing bumper crossbeam.

For the lower load path level, the subframe crossbeam did not fail in the full width test with the unmodified vehicle but its position in relation to the vehicle structure leading edge and the minimal front height limited the load applied to the barrier face. The approach taken was to maximise frontal area to distribute the applied load over a greater area of the load cell wall and to bring this structure forward to interact with the barrier face earlier in the impact and maximise its ability to absorb energy. Modification to the lower load path level was achieved by removing the existing radiator support beam, located forward of the subframe crossbeam, and fabricating a new box-section crossbeam that would take maximum advantage of the available space within the confines defined by the vehicle outer profile. This additional crossbeam would adjoin the existing subframe crossbeam at the rear (Figure 20).

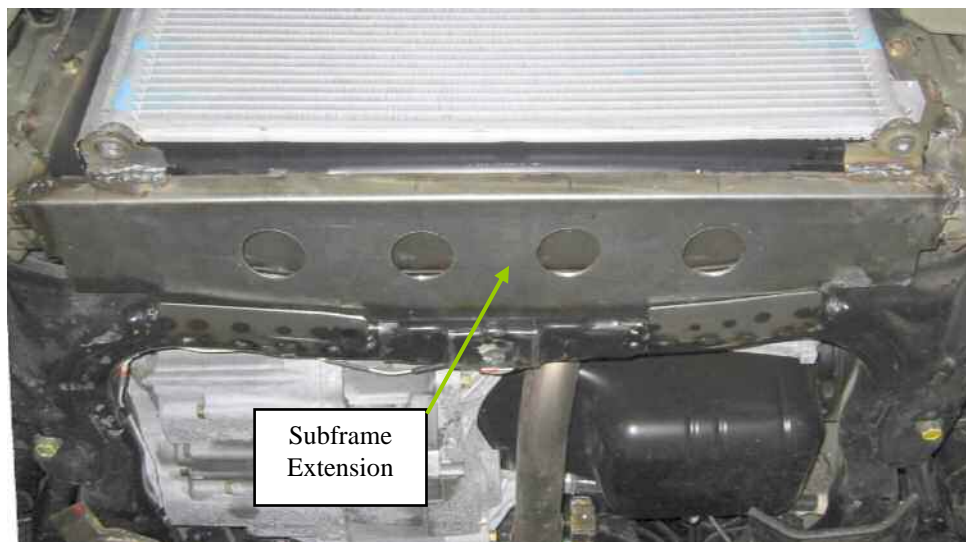


Figure 20: Subframe crossbeam extension.

For the vertical connectivity of the three fore/aft load paths, the existing connections were augmented by the additional of panels that extended forward, rearward and inboard to pick up on the strengthened slam panel and subframe extension (Figure 21). The aim was to use these additional panels to form a vertical box section beam with large cross-section that would resist the bending moment of the lateral connections between the load paths. This would also have application in an offset test and based on

this assumption additional cross bracing was incorporated into this vertical beam to increase the torsional stress.

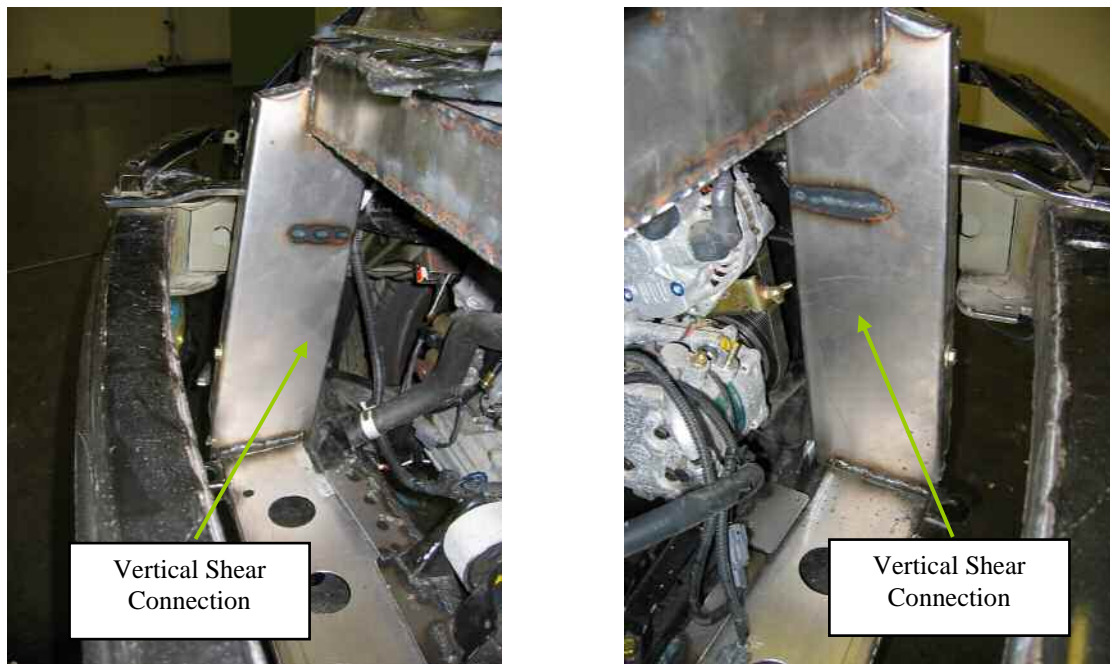


Figure 21: Improved vertical shear connection between the three fore/aft load path levels.

The above modifications were all made with a view to maintaining existing vehicle functionality. As such, all existing essential componentry of the base vehicle was retained and all modifications were contained within the existing vehicle outer profile to take into account provisions made by the manufacturer for ramp angle, aerodynamics, styling, etc. Pictures show the integration of the modifications into the test vehicle (Figure 22). The vehicle mass increase resulting from these modifications was approximately 10kg.



Figure 22: Front and underside view of the modified test car showing integration of the additional structure.

For offset impacts additional structure may be required to channel load applied to the suspension turret into the load paths around the occupant compartment.. In addition, increasing the rigidity of the front structure by introducing cross connections rearward of the vehicle leading edge would help in distributing load to the none-impact side of the vehicle. For this study, additional structure for offset impacts was not incorporated into the test vehicle

4.2 Compatibility performance assessment – FWDB test

The compatibility performance assessment of the modified test car was based on the approach defined in section 2.1 with comparison made to the performance of the unmodified test car as appropriate.

There was a difference in dynamic ride height (impact alignment) for the modified and unmodified test vehicles. The modified test vehicle impact alignment was 6 mm higher and 3 mm to the right of the unmodified vehicle impact alignment, However, this is within the estimated +/-10mm tolerance necessary for test repeatability (Thomson et al, 2005) so allowing for comparison of the load cell wall force distributions and assessment results.

The resultant load cell wall force distribution for the modified test car is shown together with the outline of the main structural members (Figure 23). As for the full width test with the unmodified car (Figure 6), the highest loads were in applied in line with the lower rail and subframe load paths; load path peak forces comparable between the two tests with the exception of the RHS subframe rail. Estimates of the load path peak forces for the modified and unmodified test cars based upon the load cell wall force distributions are detailed in Appendix A. Detailed changes in the load distribution related to the additional load applied in line with the strengthened slam panel and supporting load paths, the bumper crossbeam and the RHS subframe load path. There were increases in load path peak forces of 60%, 35% and 48% respectively.

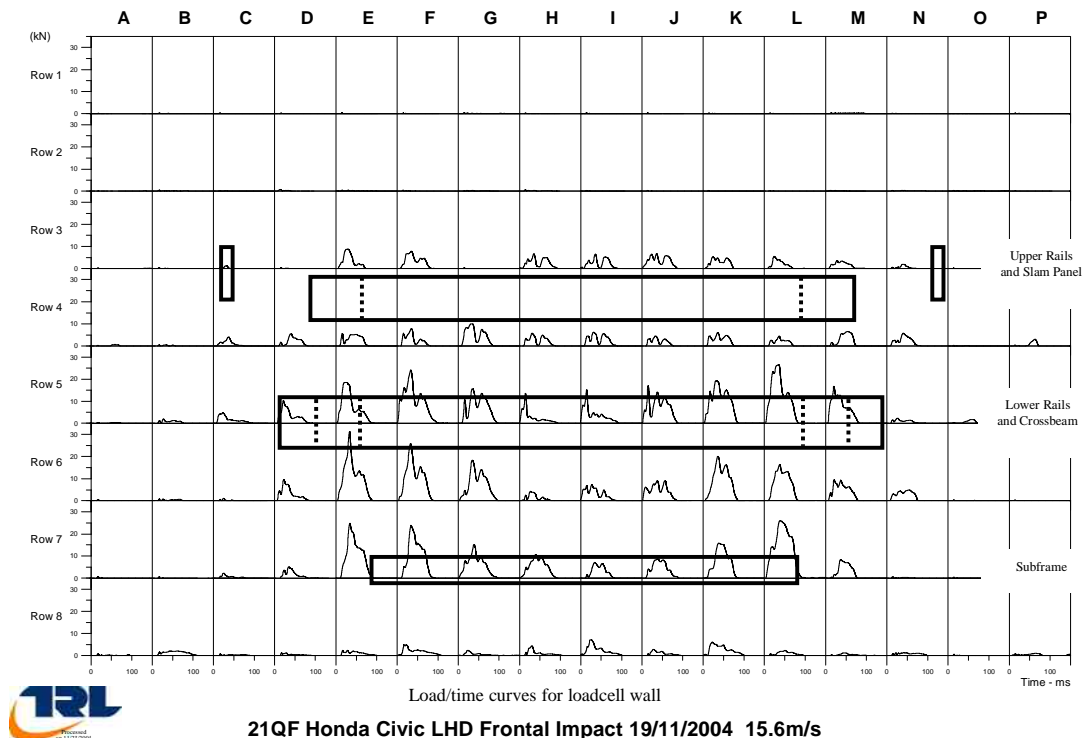


Figure 23: Force against time plot for all load cells for the modified test car showing the pre-impact alignment of the principal structural members.

The height of force over time for the modified and unmodified test cars are shown in Appendix B. Comparison between the two height of force measurements was made using the force weighted average height of force taking into account differences in static and dynamic ride height (Table 1). The force weighted average height of force was approximately 9mm higher for the modified test car due in part to the higher loads applied by the strengthened slam panel crossbeam, but were still below the lower edge height of the FMVSS part 581 bumper beam zone.

Table 1: Average HOF comparison for the modified and unmodified test cars adjusted to baseline static ride height.

	Modified Test Car	Unmodified Test Car
Average HOF	400 mm	391 mm

Homogeneity criteria based on the unsmoothed and smoothed load cell wall data set were calculated for a number of different assessment areas (Appendix C). As an objective approach to defining the assessment area has yet to be defined, for comparative purposes it has been generally accepted that an area encompassing columns 3 to 14 and rows 3 to 7 is used (C3:N7). This resulted in a higher (i.e. poorer) homogeneity criterion assessment for the modified car; 0.57 cf 0.51 (Figure 24).

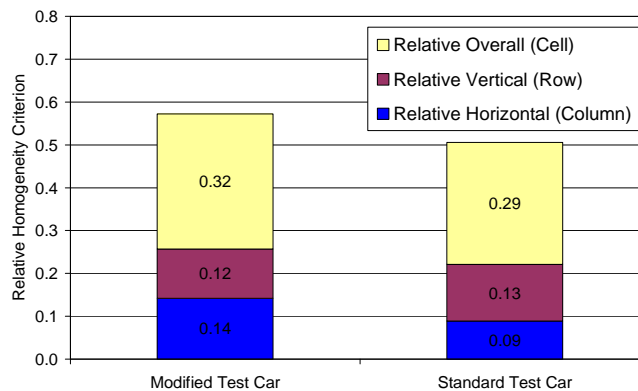


Figure 24: Comparison of relative homogeneity assessment for the modified and unmodified test cars based on assessment area C3:N7. Note that the lower the assessment value the better the force homogeneity.

However, further investigation showed that the front structure of the test car would have only partially overlapped row 3 at maximum vehicle crush. Based on height of the car front structure at the maximum crush, a more appropriate assessment area was considered to be the same width as that used previously but excluding row 3 (C4:N7) (Figure 25). This revised assessment area was used assess the change in front force homogeneity due to the modifications; the basis for the modifications to the test car was to improve front force homogeneity within the existing vehicle outer profile. The outcome is that either a variable height assessment area should be used or that a fixed height is chosen which all vehicles should load.

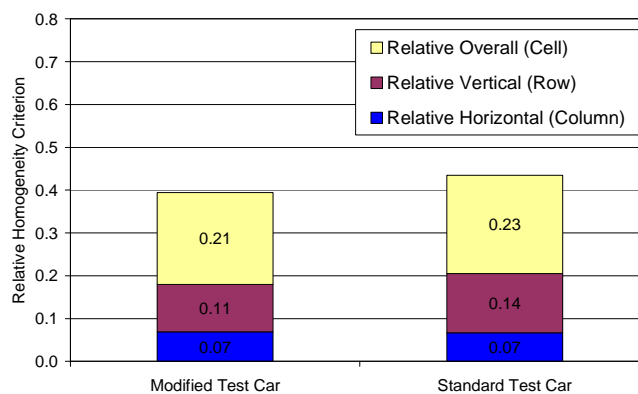


Figure 25: Comparison of relative homogeneity assessment for the modified and unmodified test cars based on assessment area C4:N7. Note that the lower the assessment value the better the force homogeneity.

It can be observed that there was an improvement in the relative homogeneity criterion for the modified test car, however this was only marginal in comparison to the differences seen in tests using other vehicles (Figure 7). The lower vertical value highlighted the increase contribution of the modified upper and subframe load path levels; row load totals at these levels 78kN cf 69kN and 151kN cf 143kN respectively (Figure 26). However, this gain was offset by the increase in load applied to row 5 by the RHS lower rail; row load total 189kN cf 153kN. Laterally there was no change in the homogeneity criteria, the increase in the measured load ahead of the strengthened crossbeam offset by the higher load measured ahead of the lower rail load paths (Figure 29).

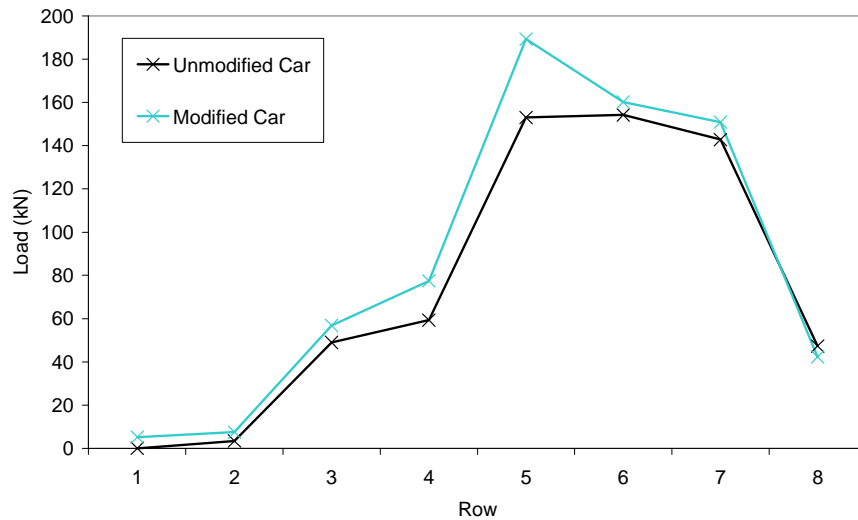


Figure 26: Peak row loads for the modified and unmodified test cars (row load based on sum of peak cell loads in that row).

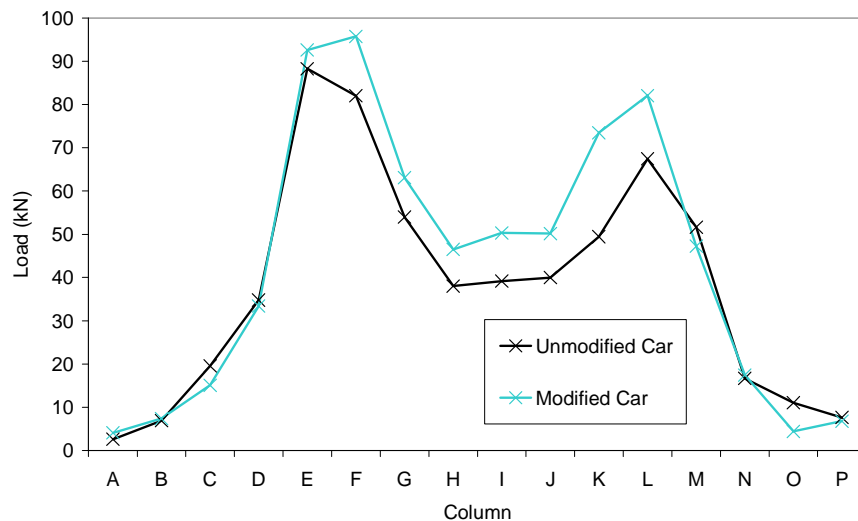


Figure 27: Peak columns loads for the modified and unmodified test cars (column load based on sum of peak cell loads in that column).

The load cell wall force is shown for both the modified and unmodified test cars (Figure 28). The modified test car was observed to have the higher load cell wall peak force and lower displacement; 560kN cf 440kN and 600mm cf 650mm. This was a consequence of the structural alterations increasing the crush strength of the vehicle front unit. Controlling the peak force level would require alterations to the existing vehicle load paths to reduce failure load. However, although this approach

was principally focused on modification through structural ‘add-ons’ such alterations to the base vehicle structure would potentially further benefit homogeneity criteria by reducing peak cell loads, especially those ahead of the lower rails; a consideration for further research work.

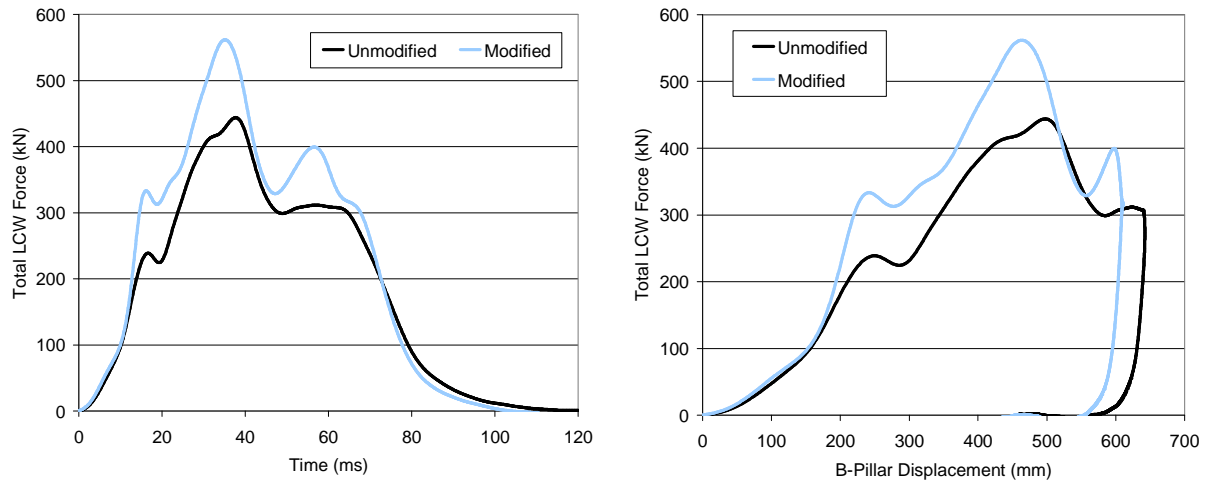


Figure 28: Comparison of total load cell wall force levels against time and displacement.

A laser scan of the deformable barrier face was performed and the result is shown (Figure 29). A similar scan was also done for the barrier face used in the test with the unmodified car so a comparison could be made (Figure 30). Observations upon comparing the two scans are that for the modified car there was greater penetration of the barrier face ahead of the extended subframe load path, the additional upper rails and the improved lower vertical shear connections. There was also a more uniform deformation of the barrier face above the bumper crossbeam level and in line with the strengthened slam panel. However, for the lower load path level there was greater penetration of the LHS lower rail and slightly less deformation ahead of the bumper crossbeam centre. It was calculated that overall barrier deformation was slightly greater for the test with the unmodified car by 0.017 m^3 ; approximately 4% of the total barrier volume. Additional images comparing maximum deformation between the two barrier faces can be found in Appendix D.

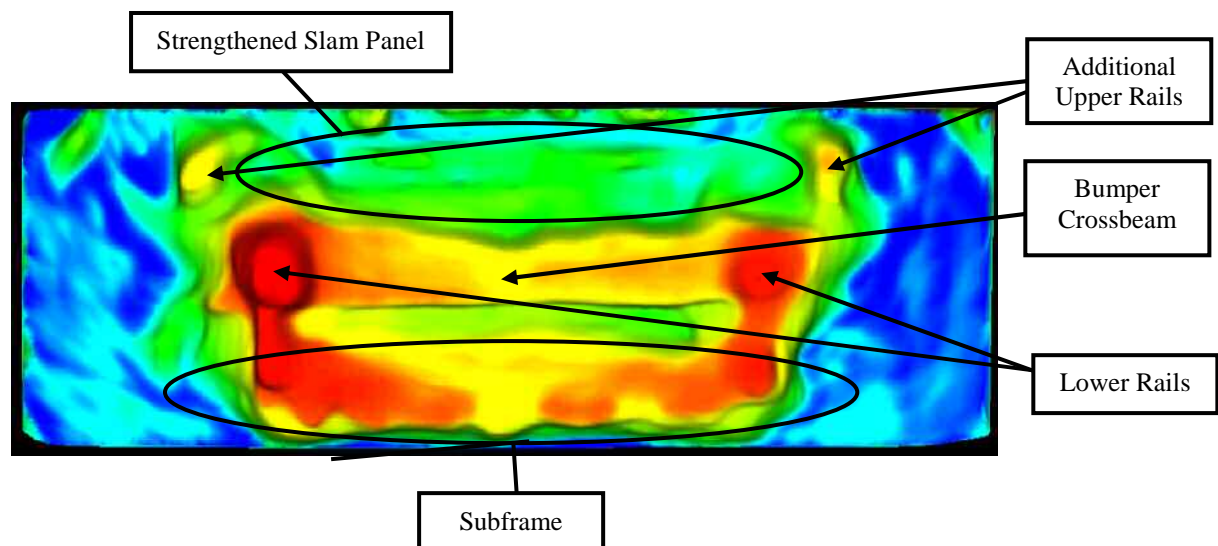


Figure 29: Scan of the deformable barrier face deformation for the test with the modified car.

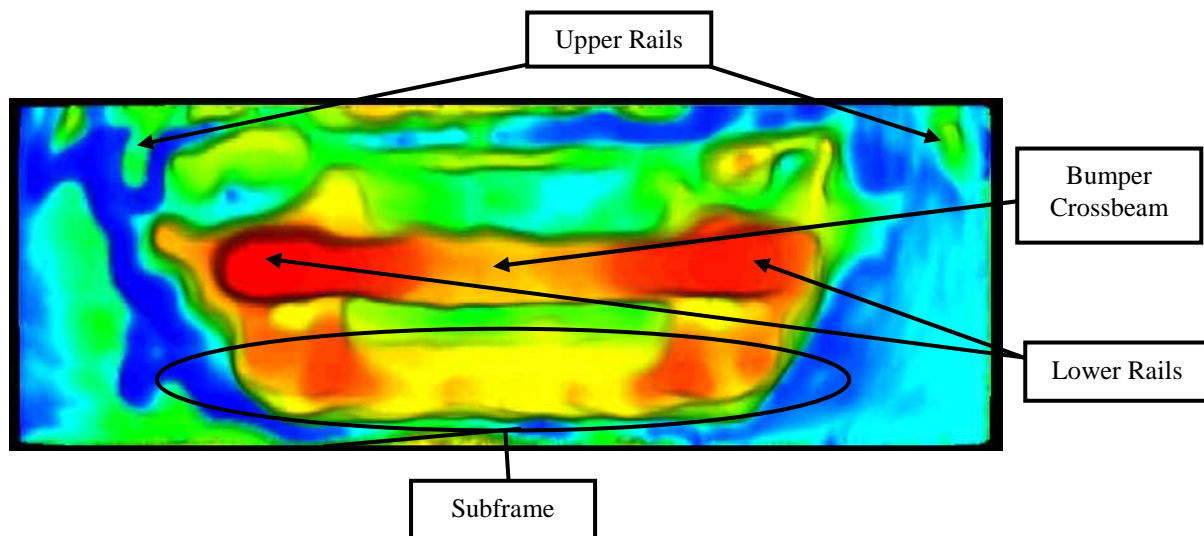


Figure 30: Scan of the deformable barrier face deformation for the test with the unmodified car.

Examination of the deformed structure of the modified test car showed both inboard upper load paths to have failed principally in axial crush with some rotation of the leading edge towards the vehicle centre due to bending moment inferred by the loading of the slam panel (Figure 31). Deformation of the existing outboard upper rails was similar to that of the unmodified test car discussed previously (Figure 10), the rails being too far rearward to interact effectively with the deformable barrier face.



RHS



LHS

Figure 31: Upper load path deformation showing failure in axial compression with slight rotation of leading edge towards the vehicle centreline.

Failure of the lower rails and subframe load paths were in bending about the vertical and horizontal axes respectively (Figure 32 and Figure 33); the position of these bending failures similar to those for the unmodified test car (Figure 8 and Figure 9). However, the level of deformation for the lower rails was visually less than for the unmodified test car possibly due to the additional energy absorption of the modified upper and subframe load path levels.

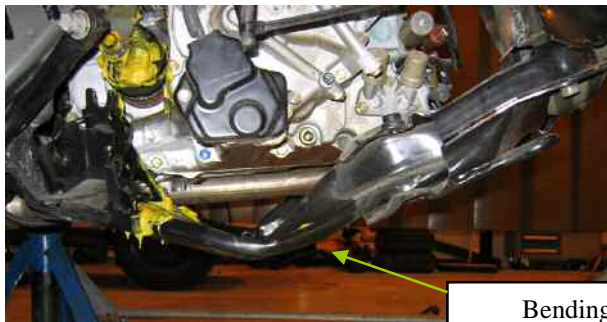


RHS



LHS

Figure 32: Lower rail load path deformation showing failure in bending about the vertical axis at different locations for the RHS and LHS. The level of deformation is visually less than for the unmodified test car.



RHS



LHS

Bending Failures

Figure 33: Subframe load path deformation showing failures in bending similar to those observed for the unmodified test car.

In terms of the lateral shear connection performance, the strengthened bumper crossbeam failed in bending with a single plastic hinge at the vehicle centreline (Figure 34). This was different from the weaker standard bumper crossbeam for the unmodified car. That failed in bending with a plastic hinge at either end just inboard of the connection to the lower rail leading edge, the centre section then displaced rearwards due to loading applied by the barrier face. Prior to failure the strengthened crossbeam was observed to apply higher load to the centre of the load cell wall; ~15kN per load cell cf ~9kN per load cell. It is believed that a better approach to increasing the bending strength of this beam may have been to increase the depth in the vehicle fore/aft direction.



Figure 34: Bumper crossbeam deformation showing the single plastic hinge failure at the vehicle centreline.

For the strengthened slam panel and subframe extension, deformation was principally in axial crush due to loading applied by the barrier face (Figure 35). The vertical shear connections between the three load path levels showed only little sign of distortion post impact but the lower part of this strengthened connection was responsible for high load applied to the wall between the lower rail and subframe load paths and the high barrier penetration mentioned previously (Figure 35).

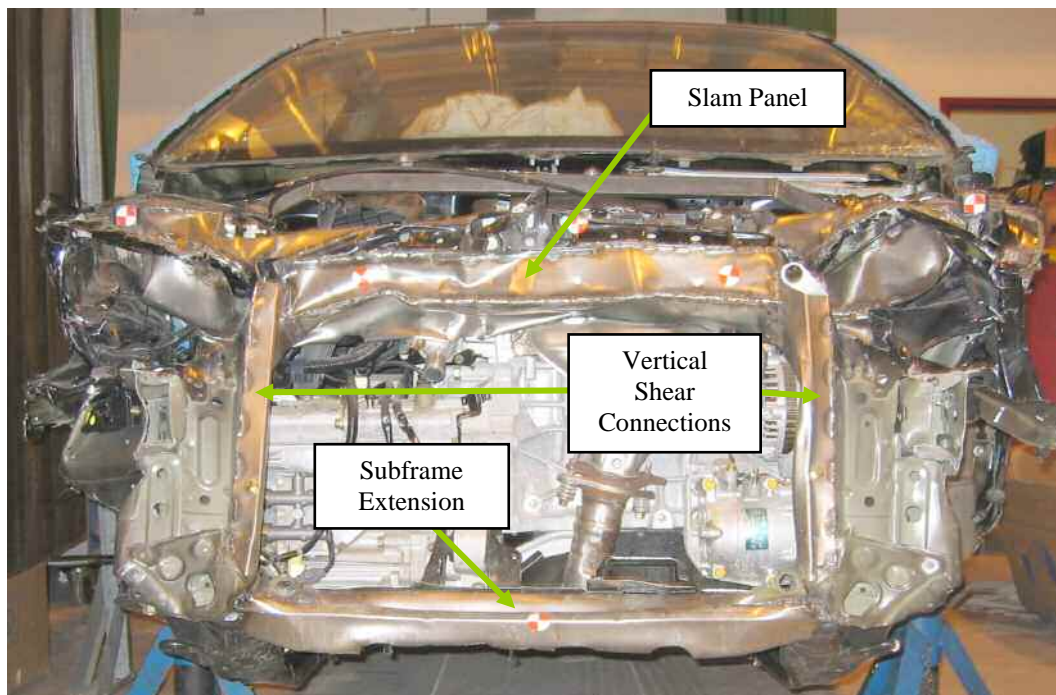


Figure 35: Front view showing slam panel, subframe extension and vertical shear connections post impact (bumper crossbeam and radiator removed).

For the self-protection afforded to the occupants, the full width test configuration generates a high occupant compartment deceleration pulse that is especially demanding of the restraint system. The compartment deceleration pulse for the modified and unmodified vehicles was observed to be in general comparable, with a slightly lower final peak for the modified vehicle (Figure 36). The interaction of the additional structure with the barrier face was the probable cause of the additional peaks noted in the compartment deceleration of that car at 18ms and 32ms. However, the airbag firing time was observed to differ significantly, the firing time for the unmodified test car 25.5ms and for the modified test car 10.5ms. In comparison with other vehicles subject to the full width test it was considered that the firing time for the unmodified vehicle was late and was a contributory factor in the high chest loading previously noted in the assessment of that vehicle.

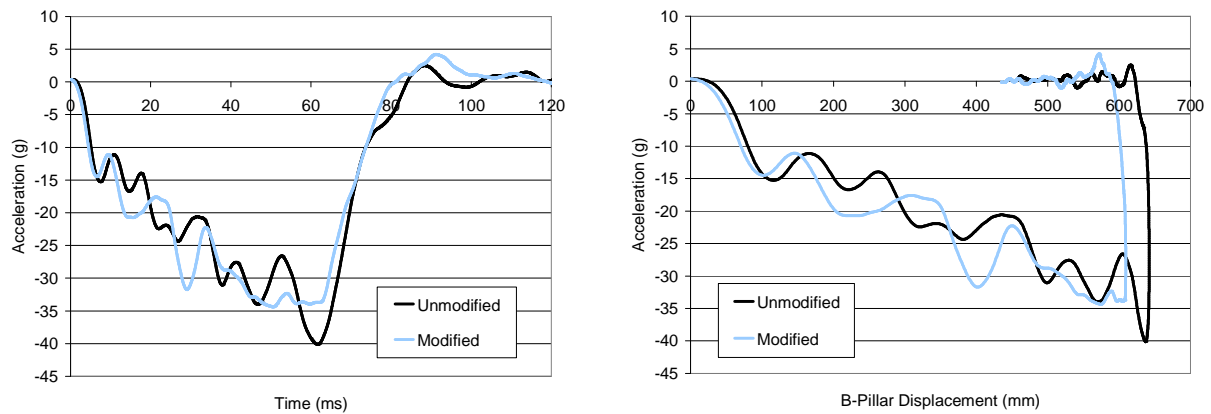


Figure 36: Comparison of compartment accelerations for the modified and unmodified test cars.

In terms of the self-protection, all the dummy injury criteria were below the ECE Regulation 94 injury limits (Figure 37). For the majority of the injury criteria the levels were in general equal to or slightly less than those of the unmodified test car, showing that the increase in frontal crush strength of the vehicle front unit had no detrimental effect on self-protection levels in this impact configuration.

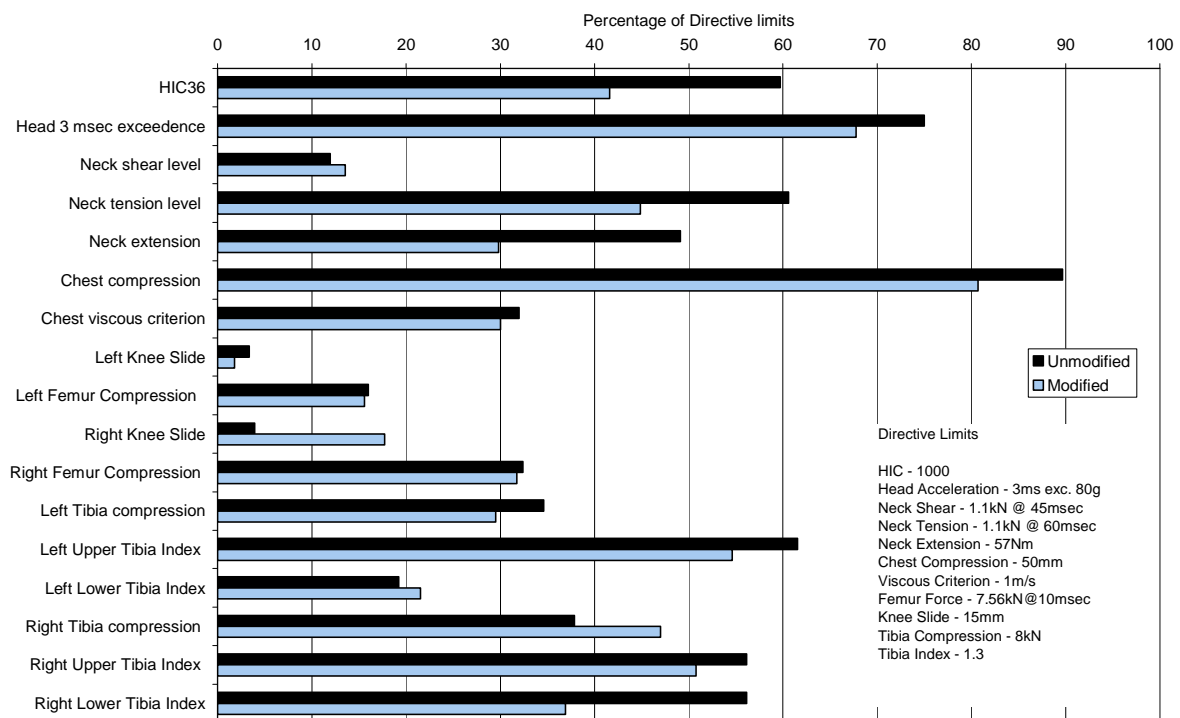


Figure 37: Comparison of dummy results for the modified and unmodified test cars.

4.3 Improvement of test car compatibility performance summary

The modifications to the test car consisted primarily of additional upper load paths set inboard of the existing upper load paths and connected across the front of the vehicle by a strengthened slam panel structure. At the lower rail level, the existing bumper crossbeam was reinforced with a closing panel along the rear edge to increase load contribution cross the vehicle front. At the subframe level the existing crossbeam structure was augmented with a box section beam to act as an extension and provide greater interaction area increase energy absorption capability. Improvements were also made

in vertical connectivity between the load path levels although these were believed to have greater relevance to offset impact configuration; the connections not observed to have failed in the previous test with the unmodified car.

Based upon the performance of the modified test car in the FWDB test configurations the following conclusions can be made regarding the improvement in the compatibility performance:

- There was an increase in the average height of force by 9mm due to the addition structure and an improvement in the relative homogeneity measure. However, the latter was based on an assessment different to that considered in the initial assessment of the unmodified test car. This was due to the car at maximum crush only partial loading the upper row of load cells in the original assessment area. The assessment area was therefore revised as the aim of this assessment was to improve force homogeneity within the existing vehicle frontal outline. In assessing crash compatibility it will be necessary either to have a variable height assessment area or a fixed assessment area height that all vehicles should load.
- There was a higher peak load cell wall force for the modified car. This was as a consequence of the structural ‘add-ons’ increasing the crush strength of the vehicle front unit. Reducing the crush strength would require alterations to the existing load paths to reduce their crush strength. Although such alterations were not considered as part of this research it is likely that such reduction would result in additional improvement to the front force homogeneity and hence the relative homogeneity criterion metric based upon this force distribution.
- The modifications to the upper load path level were successful in increasing the applied load; an increase in the peak load of 68%. The additional structure was observed to have failed principally in axial crush therefore maximising potential additional energy absorption. This was observed to have improved the vertical force homogeneity measure. The failure load of the additional upper rails was lower than that of the supporting structure. However in an offset test the vehicle crush is greater and both the additional and existing upper rail load paths would load the supporting structure. This may require reinforcement of the supporting structure.
- The increase in the bending strength of the bumper crossbeam was successful in increasing the load contribution ahead of the centre of this beam; an increase in the peak load of 35%. However, this was countered by the increase in the measured ahead of the lower rail load paths when assessing lateral homogeneity. In addition, once the bumper crossbeam had failed, loads ahead of the crossbeam on the modified car were less that they had been on the unmodified car. This resulted from the different failure modes; a single bending failure at the centre for the modified car and two bending failures, one at either end of the crossbeam, in the test with the unmodified car.
- The subframe extension was successful in applying load earlier in the impact improving the vertical force homogeneity and absorbing additional impact energy through failure in axial crush. Load increase at this level was restricted to the RHS subframe load path level due to the additional stability added by the improved vertical shear connections; an increase in the peak load of 48%.
- The structural deformation of the existing load paths was observed to be relatively unaffected by the modifications with the exception of the bumper crossbeam which failed with a single plastic hinge at the beam centre. It is believed that a better approach to increasing the bending strength of this beam may have been to increase the depth in the fore/aft vehicle direction. The principal failure mode of the additional structure was in axial crush.
- Regarding the self-protection performance, occupant compartment acceleration was comparable between the two cars, but there was significant difference in the firing times of the restraint system, that of the unmodified car considered late in relation to other vehicles tested in this configuration. The occupant injury criteria were in general similar or slightly less for the modified vehicle.

5 Concept Modelling Technique Development

For concept development a model should be able to be changed quickly and easily and require little computer CPU time so that many simulations can be performed. Full scale Finite Element (FE) models are not ideally suited to this as they have large CPU requirements and alterations to the model can sometimes be time consuming. To overcome these problems smaller concept type FE models can be used, which use beam elements to represent the car's main structural members and shell elements with a coarse mesh to represent the large panels (Figure 38). Although this type of concept model is not as accurate as a full scale FE model, it is simple to alter and computationally inexpensive. However, to be able to use it, an efficient way to estimate the beam element properties is required.

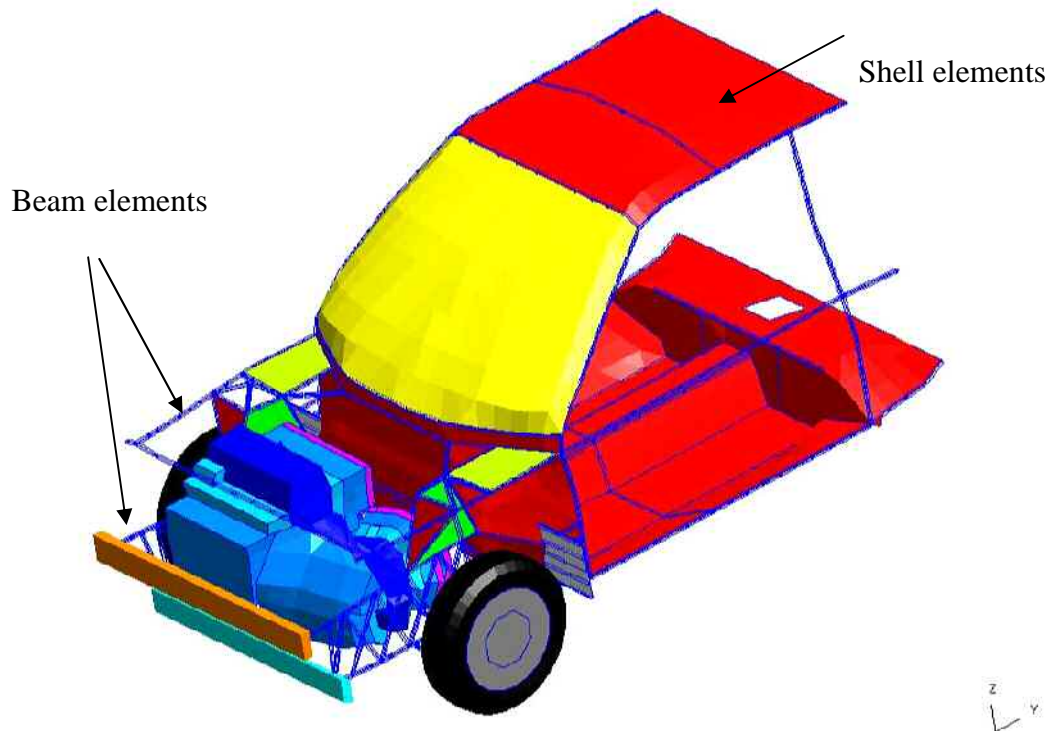


Figure 38: Concept model showing extensive use of beam elements.

The 'MAT_MODIFIED_FORCE_LIMITED' material model in the LS-DYNA (Oasys/Arup) software represents a beam's plastic properties using a non-linear translational spring for axial crush and non-linear rotational springs for plastic bending. The reduction in a section's bending moment strength under axial loading is also represented by making the beam's plastic bending properties a function of the axial load. This technique is referred to as 'load mode coupling', and is important when modelling car structures which are subjected to high axial loads. A tool based upon a number of mathematical relationships has been developed to estimate the beam element properties of a section and translate them into a format suitable for input into the 'MAT_MODIFIED_FORCE_LIMITED' material model in a LS-DYNA input deck. This tool can also be used to estimate possible section sizes for given axial crush and bending moment requirements. The development and validation of the methodology on which this tool is based is described.

5.1 Development of the methodology

5.1.1 Axial loading

Under axial load, a thin-walled member will fail either in axial crush or in Euler buckling. Whether it will fail in axial crush or in buckling is determined by its slenderness ratio. In axial crush the difference between the critical stress of the section and the material's yield stress will determine whether the member will crush regularly or irregularly. A regular fold is preferable as irregular folds will induce bending moments, possibly causing the whole columns to fail in bending, hence absorbing less energy. The critical stress value depends on the smallest t/b ratio of the section, where t is the thickness and b the width of the buckling (largest) plate.

When a tube is crushed axially, the force versus strain characteristic has two main features; the peak load and the mean load. The peak load value determines the force needed to trigger the collapse mechanism. Its value is determined by the stress concentration in the section's edges. The mean load determines the amount of energy the member will be able to absorb by crushing (Mahmood et al, 1981). For a rectangular section, the peak load is always greater than the mean load (between two and ten times). For a circular section, the peak and mean load will have very similar values.

For the current methodology, the mean load is calculated using an empirical formula. The peak load is estimated as being twice this value. This simplification is based on the assumption that automotive structures rarely behave as compact ones. Automotive structures have indentations, pressing defaults and holes for component fitting, and are spot-welded. These defects will reduce the peak load substantially. The formula used to estimate the mean load in the current methodology was determined experimentally (Magee et al, 1978) using square steel columns. The formula gives reasonable results for the range ($0.008 < t/b < 0.025$) which is typical for automotive structures:

$$P = 4.25A\left(\frac{t}{b}\right)^{0.8}\sigma_{ult}$$

P : mean load

A : cross sectional area

t : thickness

b : width of buckling plate

σ_{ult} : ultimate stress

The maximum engineering strain value used for crush was the experimentally determined average value of 0.728 (Abramowicz, 1983). Further strain compresses the material of the thin walled member.

5.1.2 Pure bending

Plastic bending is initiated by buckling of one of the section's panels. Depending on the difference between critical stress and yield stress, three types of failure can be obtained; elastic buckling, plastic buckling or mixed mode. Semi-empirical formulae exist for these three types (Belingardi et al, 2000)). The idealisation process used in the current methodology calculates the critical stress and uses the following equation to estimate the initial plastic bending moment, which gives a compromise between the three possible failure types:

$$M_{p0} = C \cdot \frac{\sigma_{cr} + \sigma_y}{2} \cdot I_p$$

M_{p0} : plastic bending moment

C : shape factor determined experimentally (0.93 recommended for rectangular sections)

σ_{cr} : critical stress

σ_y : yield stress

I_p : primary moment of inertia.

Another critical point regarding bending of thin-walled tubes is the jamming angle (angle for which buckling walls contact inside a plastic hinge). When the plastic hinge's angle exceeds this value, its moment may start increasing again or continue decreasing, depending on the section's shape, its orientation and the material's thickness (Keckman, 1983; Kim et al, 2001). Practical experiments rarely reach the jamming angle. To overcome this lack of experimental data, many detailed finite element simulations were carried out for a range of sections typical of automotive structures. From these an average plastic bending characteristic was determined. The ratio between the plastic moment and the initial plastic moment was estimated for various angular values. An artificial lock up occurs at $\Theta=90^\circ$ to maintain model stability and limit the amount of energy a hinge can absorb.

5.1.3 Load mode coupling

Practically, when any member is loaded axially as well as in bending, the value of the initial plastic bending moment is decreased compared to when it is not loaded axially (Keckman, 1981). The material model used in LS-DYNA uses coupling tables to represent this effect. Detailed finite element simulations of sections loaded simultaneously axially and in bending were carried out to develop a coupling curve. Another curve was also derived using the fully plastic theory equation shown below:

$$\left(\frac{M}{M_{p0}} \right) + \left(\frac{P}{P_m} \right)^2 = 1$$

M : plastic bending moment

M_{p0} : initial plastic bending moment

P : Axial load

P_m : Mean crush load

Comparison of these curves shows close agreement except at high axial loads (Figure 39).

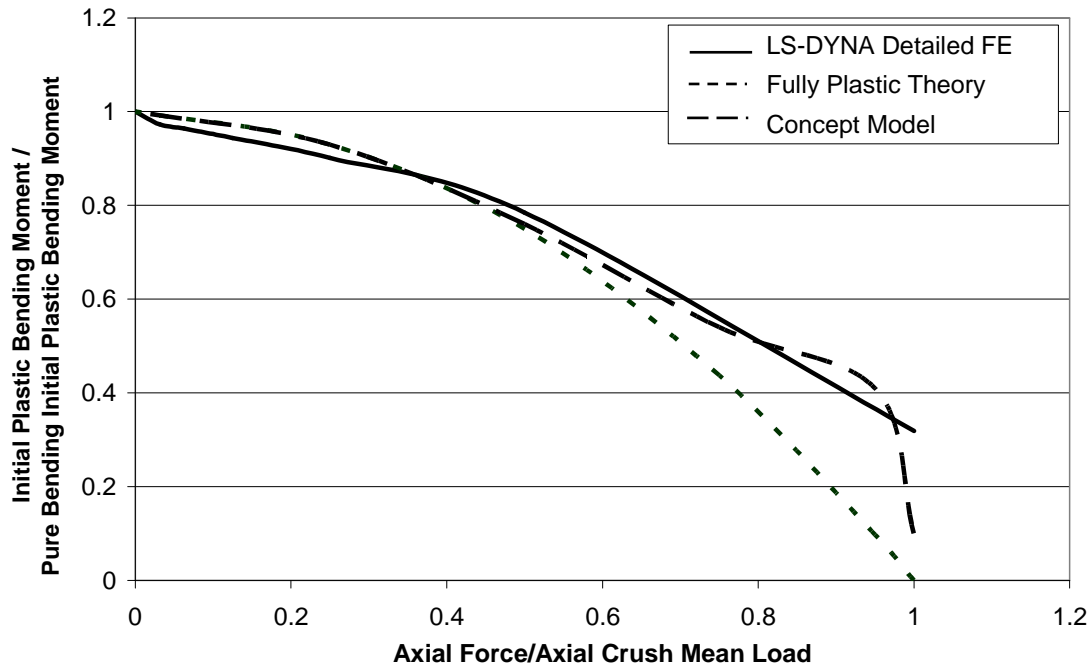


Figure 39: Comparison of coupling curve used in the concept methodology with those derived.

5.2 Validation of the methodology

To validate the methodology experimental results were compared with predicted results. However, as not many experimental results could be found in the literature, the methodology was further validated using detailed FE simulations to generate more data for axial crush and pure bending loading conditions. All the simulations were performed at low speed (5m/s). In reality structures may deform differently when impacted at high speed as inertial effects and strain hardening can become significant.

5.2.1 Axial crush

The prediction of the mean crush force was reasonable for rectangular sections with a t/b ratio between 0.007 and 0.02 (Figure 40). However, the prediction of the initial peak load was not as good. Realistically, while the peak load under quasi-static test conditions is fairly repeatable, under dynamic loading conditions the peak load of automotive sections will be extremely sensitive to parameters such as the impact speed and material defects. Therefore even detailed FE simulations would not be very reliable in estimating peak load.

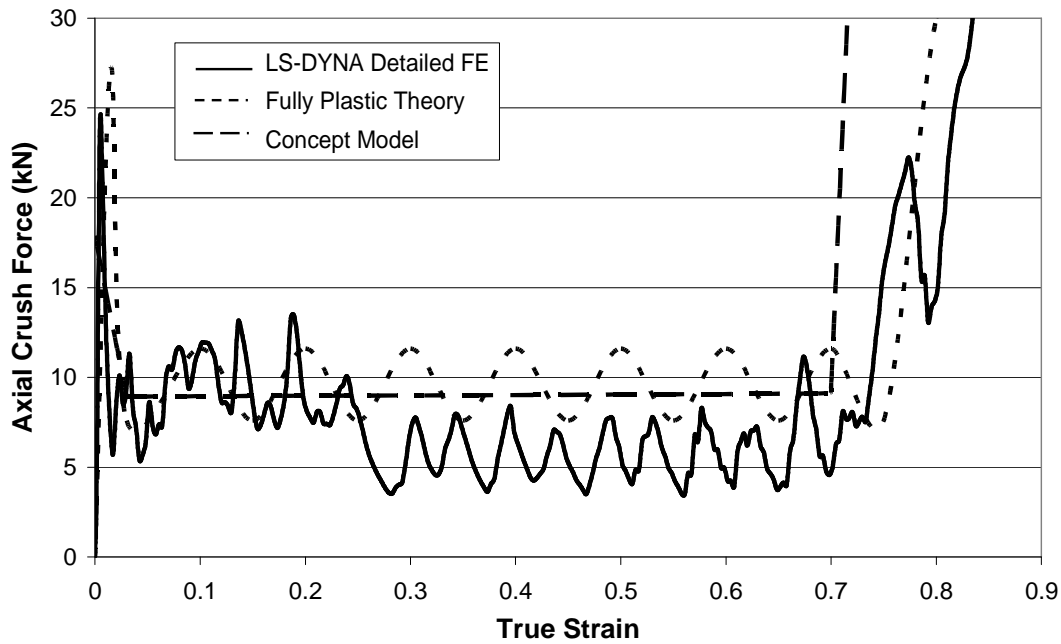


Figure 40: Load vs Strain curve for axial crush showing comparison between experiment and detailed FE and concept methodology predictions.

5.2.2 Pure bending

The prediction of the initial plastic bending moment compared well with the experimental data and the detailed FE simulation (Figure 41). However, past the initial value, the predictions are not so good. For the case shown the bending moment is initially under estimated and later over estimated. In addition, the methodology always predicts a rise of the bending moment value past the jamming angle, which is incorrect as this is dependent on the height / width ratio of the section. However, it is even difficult to model this effect accurately using detailed FE simulation unless a very fine mesh is used. Past the concept stage, once a reliable detailed finite element model is developed, this problem should be addressed.

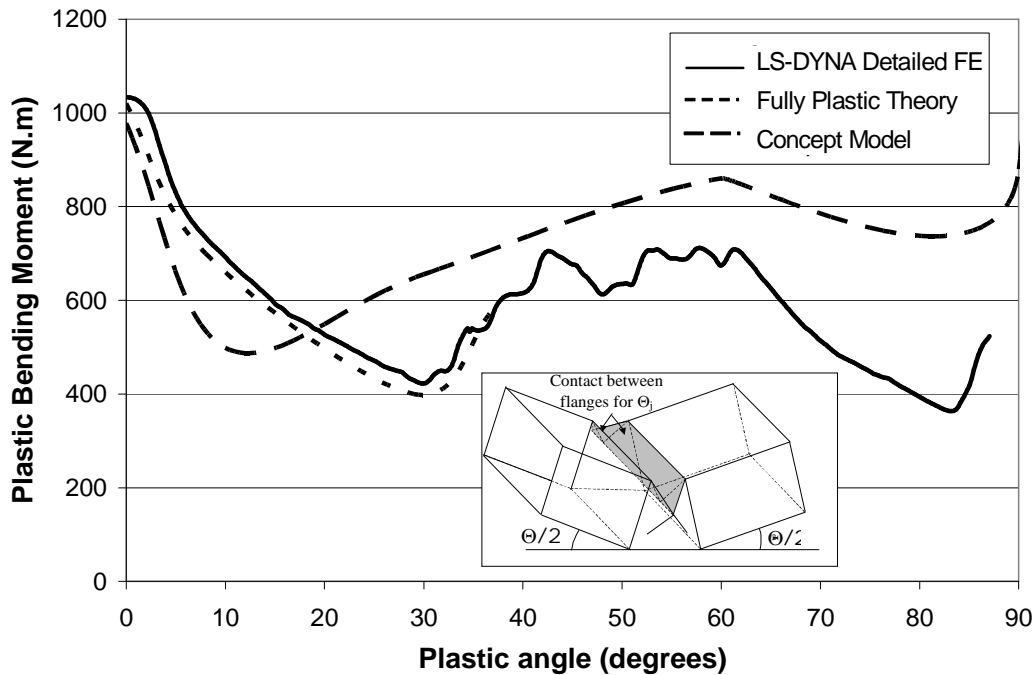


Figure 41: Plastic moment vs plastic angle curve for pure bending load showing comparison between experiment and detailed FE and concept methodology predictions.

5.3 Concept model development summary

For initial concept design type studies models are required that are simple to alter and computationally inexpensive. Simple FE models that use beam elements to represent a car's main structures are suitable for this type of work. A tool to estimate the beam element properties of a section and translate them into a format suitable for input into the 'MAT_MODIFIED_FORCE_LIMITED' material model in a LS-DYNA input deck has been developed. This tool can also be used to estimate possible section sizes for given axial crush and bending moment requirements. However, it should be noted that the methodology on which this tool is based has only been validated for a limited range of section sizes and shapes, i.e. simple thin walled rectangular and square sections with a t/b ratio between 0.007 and 0.02, where t is the thickness and b the width of the buckling (largest) plate.

6 Conclusions

A proposal to assess and investigate vehicle compatibility performance focuses on a suite of three car-to-barrier tests, each test measuring one aspect of the compatibility performance; structural interaction, front force level matching and compartment strength. The approach to assess car compatibility performance defined as part of the research reported here builds upon this current proposal by detailing a number of additional analyses that would help to understand and identify the reasons for a particular car's compatibility performance measurement. The outcome is a methodology that provides both compatibility performance assessment and recommendations for improvement. However, as these tests have yet to be completely validated, the approach contains additional car-to-car tests that can be used to confirm the findings of the car-to-barrier tests.

The above approach was applied to a test vehicle. Regarding the structural interaction potential, the principal finding was that although there was a reasonable balance between the loads applied by the lower rails and subframe load paths to attain good vertical force distribution the load applied by the upper load path should be increased. For the frontal force level, this was found to be comparable to other vehicles of similar mass. Whilst the self-protection level (the protection afforded to the vehicle

occupant) was found to be in accordance with current ECE regulations for frontal impact, it was noted that the driver chest loading in the full width barrier test was high due to contact with the steering wheel. Principal recommendations from this assessment were that the load contribution from the upper load path level should be increased to improve structural interaction potential, that any structural modifications should ideally limit increases in frontal force level to prevent the car becoming too stiff in relation to cars of similar mass and that consideration should be given to altering the restraint timing to lower the driver chest loading.

Modification of the test car was undertaken with the aim of improvement in structural interaction as assessed in the FWDB test configuration because structural interaction is the prerequisite for improved compatibility performance. The modifications were of the 'add-on' type and incorporated into the existing car so that they had minimal effect upon the existing car functionality. These structural add-ons consisted of additional upper rails located inboard of the existing rails, a strengthened slam panel crossbeam, strengthened bumper crossbeam and a subframe load path extension. Improvements were also made to the vertical connectivity between the load path levels. These modifications aimed to improve the frontal force distribution of the test car without prejudicially affecting frontal force level or self-protection.

Assessment of the modified test car in the FWDB test showed the upper load path level modifications to be successful in increasing the applied load, resulting in an improvement in the vertical force homogeneity. However, whilst there was an increase in the measured load ahead of the centre of the strengthened bumper crossbeam, higher loads ahead of the lower rail / subframe load paths negated any improvement in lateral force homogeneity. For the subframe load path, the extension was successful in loading the barrier and absorbing impact energy through axial crush. Regarding the frontal force level, there was an increase in the peak load measured by the load cell wall although this did not overload the occupant compartment in this test configuration. However, consideration needs to be given to the additional load that would be applied to the compartment at waist level in an offset impact when both the existing and additional upper rail load paths would be simultaneously loaded – the existing upper load path was too far rearwards in the full width impact to apply a significant load to the occupant compartment. For the self-protection, the occupant compartment deceleration pulses were similar for the modified and unmodified vehicles. However, the airbag firing times differed significantly, that for the unmodified car considered to be late when compared with other vehicles tested in this configuration. Actual dummy injury criteria were in general similar or slightly lower for the modified test car.

The results of the above investigation demonstrate the suitability of the compatibility performance assessment for improving car compatibility performance. However, further work would be required to demonstrate improved compatibility performance of the test car in other impact configurations in addition to the full width test discussed here.

Concept modelling allows for structural integration of cars to be investigated at the concept design stage. A tool to estimate the beam element properties of a section and translate them into a format suitable for input into the mathematical modelling software was developed. This tool can also be used to estimate possible section sizes for given axial crush and bending moment requirements. However, it should be noted that the methodology on which this tool is based has only been validated for a limited range of section sizes and shapes, i.e. simple thin walled rectangular and square sections with a t/b ratio between 0.007 and 0.02, where t is the thickness and b the width of the buckling (largest) plate.

7 Acknowledgements

The work described in this paper forms part of a Transport Research Foundation (TRF) funded research project performed by TRL Limited. The author gratefully acknowledges the contribution of the Honda R&D Europe in donating two test vehicles for the experimental investigations.

8 References

- ABRAMOWICZ W, (1983). The effective crushing distance in axially compressed thin-walled metal columns. *Int. J. of Impact Engineering.*, Vol. 1, No. 3, pp. 309-317, 1983.
- BELINGARDI G, GUGLIOTTA A, MONTANINI R, AND VADORI R, (2000). Element formulation to simulate the localised plastic collapse in the crash analysis by multibody approach. *European Congress on Computational Methods in Applied Sciences and Engineering*, 2000.
- DELANNOY P, AND JACQUES F, (2003). Compatibility Assessment Proposal Close From Real Life Accident. *Eighteenth International Technical Conference on the Enhanced Safety of Cars*, Nagoya 2003. Paper number 94.
- DIBOINE A, AND DELANNOY P, (2002). Improvements in Car-to-car Compatibility: Physics, Design Constraints and Assessment Test Methodology and Criteria. *Car Safety 2002 Conference*, London, UK, June 2002.
- ECE (United Nations) Regulation 94, Uniform Provisions Concerning the Approval of Vehicles with Regard to the Protection of Occupants in the Event of a Frontal Collision.
- EDWARDS M, HAPPIAN-SMITH J, BYARD N, DAVIES H, AND HOBBS A, (2000). Compatibility – The Essential requirements for cars in frontal impact. *Car Safety 2000 conference*, London, UK, June 2000.
- EDWARDS M, HAPPIAN-SMITH J, DAVIES H, BYARD N AND HOBBS A, (2001). The Essential Requirements for Compatible Cars in Frontal Collisions. *Seventeenth International Technical Conference on the Enhanced Safety of Cars*, Amsterdam 2001.
- EDWARDS M, DAVIES H, AND HOBBS A, (2003). Development of Test Procedures and Performance Criteria to Improve Compatibility in Car Frontal Collisions. *Eighteenth International Technical Conference on the Enhanced Safety of Cars*, Nagoya 2003. Paper Number 86.
- H.S KIM, T WIERZBICKI, “Crush behaviour of thin-walled prismatic columns under combined bending and compression”, *Computers and Structures*, vol. 79, pp. 1417-1432, 2001.
- KECMAN D, (1983). Bending collapse of rectangular and square section tubes. *Int. J. Mech. Sci.* Vol 25, No. 9 10, pp. 623-636, 1983.
- KECMAN D, (1981). Program West for optimization of rectangular and square section tubes from the safety point of view. *SAE paper 811312*, 1981.
- MAGEE C L, AND THORNTON P H, (1978). Design Considerations in Energy Absorption by Structural Collapse. *SAE Paper No. 780434*, 1978.
- MAHMOOD H F, AND PALUSZNY A, (1981). Design of thin-walled columns for crash energy management, their strength and mode of collapse. *SAE paper 811302*, 1981.
- OASYS / ARUP. LS Dyna Environment. <http://www.arup.com/dyna/>
- O'REILLY P, (2001). Status Report of IHRA Car Compatibility Working Group. *Seventeenth International Technical Conference on the Enhanced Safety of Cars*, Amsterdam 2001. Paper Number 337.
- SUMMERS S, HOLLOWELL W T, AND PRASAD A, (2002). Design Considerations for a Compatibility Test Procedure, *Society of Automotive Engineers*, Paper No. 2002-02B-169, March 2002.
- THOMSON R, AND EDWARDS M, (2005). Passenger Vehicle Crash Test Procedure Developments in the VC-Compat Project. *Nineteenth International Technical Conference on the Enhanced Safety of Cars*, Washington 2005. Paper number 05-0008.

-
- VC-COMPAT PROJECT (2003). Full Width Deformable Barrier Protocol v1.3. <http://vc-compt.rtdproject.net>.

Appendix A: Load Path Impulse and Peak Forces

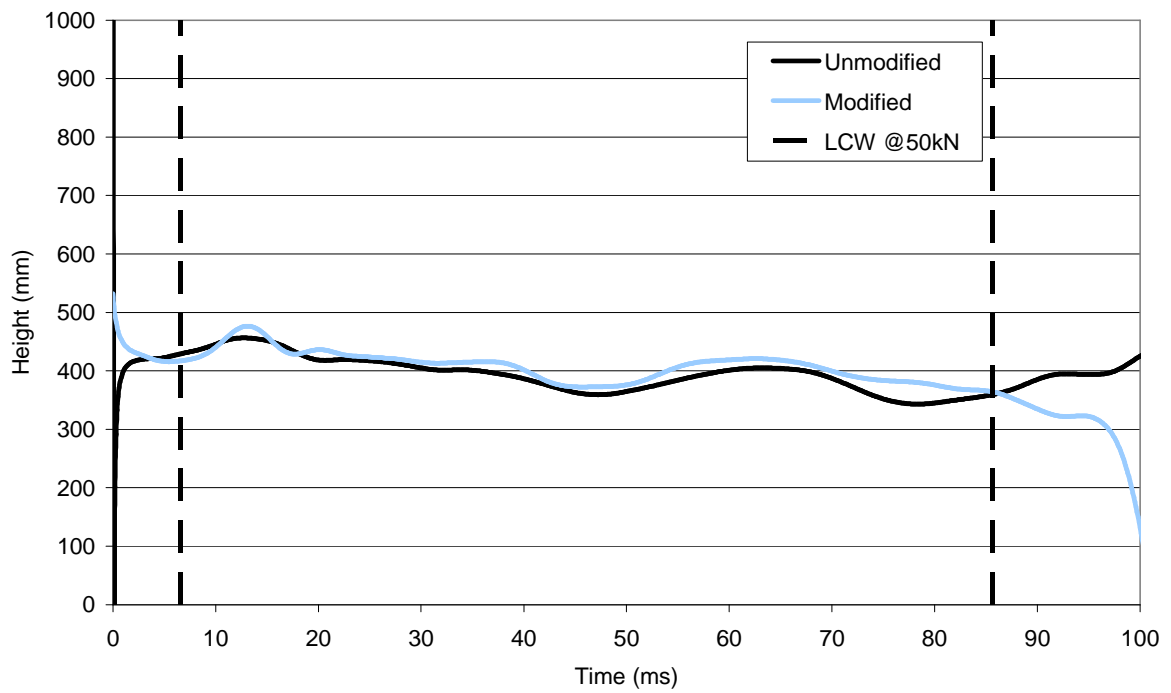
Unmodified Test Car

	Load Area	Impulse Ns	Peak Force	
			Force – kN	Time - ms
LHS Lower Rail	D5:E6	1724	61.8	29.6
RHS Lower Rail	L5:M6	2264	63.3	29.7
LHS Upper Rail	C3:D3	193	6.61	41.3
RHS Upper Rail	M3:N3	152	6.57	41.1
Slam Panel	D4:M4	1823	36.16	28.8
LHS Subframe Crossbeam/Load Path	E7:F7	1594	48.7	37.2
RHS Subframe Crossbeam/Load Path	K7:L7	1223	28.2	40.7
Subframe Crossbeam	G7:J7	1857	40.1	40.0
Engine + Bumper Beam	F5:K6	5651	116.4	37.2
LCW	A1:P8	21527	443.9	37.7

Modified Test Car

	Load Area	Impulse Ns	Peak Force	
			Force - kN	Time - ms
LHS Lower Rail	D5:E6	2261	62.55	33.10
RHS Lower Rail	L5:M6	2815	64.09	36.60
LHS Upper Rail	C3:D3	107	4.74	34.5
RHS Upper Rail	M3:N3	242	7.68	40.1
Slam Panel	D4:N4	2264	57.09	36.2
LHS Subframe Crossbeam/Load Path	E7:F7	1772	48.74	34.30
RHS Subframe Crossbeam/Load Path	K7:L7	1955	41.77	38.40
Subframe Crossbeam	G7:J7	1699	40.87	38.5
Engine + Bumper Beam	F5:K6	7429	157.64	34.70
LCW	A1:P8	24638	561.73	35.20

Appendix B: Height of Force



Appendix C: Variance and Homogeneity Criteria

09PF Honda Civic

LCW Maxima - Variance and Homogeneity criteria

First Column	Last Column	First row	Last row	Target (max) load kN	Average (max) load kN	Cell Variance	Row Variance	Column Variance	Target Criterion	Cell homogeneity criterion	Row homogeneity criterion	Column homogeneity criterion	Overall homogeneity criterion	Relative homogeneity criterion
2	15	3	8	7.2	7.1	42.3	12.5	15.9	0.0	42.3	12.5	16.0	70.8	1.347
3	14	3	8	8.5	8.0	43.0	16.4	12.5	0.2	43.2	16.6	12.7	72.5	1.013
2	15	4	8	8.7	7.8	46.7	11.6	21.2	0.8	47.4	12.4	22.0	81.8	1.080
3	14	4	8	10.1	8.9	46.9	15.5	17.4	1.7	48.6	17.2	19.1	85.0	0.825
4	13	4	8	12.2	10.0	48.1	22.5	12.9	4.7	52.8	27.2	17.7	97.7	0.659
2	15	3	7	8.7	7.9	46.5	11.4	21.1	0.7	47.2	12.1	21.8	81.1	1.072
3	14	3	7	10.1	8.9	46.0	14.8	16.7	1.5	47.5	16.3	18.2	82.0	0.796
4	13	3	7	12.2	10.1	47.0	21.6	12.0	4.4	51.4	26.0	16.3	93.7	0.632
3	14	4	7	12.7	10.2	48.8	10.4	25.1	6.2	55.1	16.7	31.3	103.0	0.640
4	13	4	7	15.2	11.6	47.0	15.9	18.6	13.3	60.3	29.2	32.0	121.5	0.524

Unsmoothed data

First Column	Last Column	First row	Last row	Target (max) load kN	Average (max) load kN	Cell Variance	Row Variance	Column Variance	Target Criterion	Cell homogeneity criterion	Row homogeneity criterion	Column homogeneity criterion	Overall homogeneity criterion	Relative homogeneity criterion
2	15	3	8	6.4	7.3	23.0	6.3	11.8	0.9	23.9	7.1	12.7	43.7	1.064
3	14	3	8	7.5	8.3	20.7	8.8	7.5	0.7	21.4	9.5	8.3	39.2	0.701
2	15	4	8	7.7	8.3	23.9	3.2	17.9	0.4	24.3	3.6	18.2	46.1	0.780
3	14	4	8	9.0	9.5	19.3	4.5	12.2	0.2	19.6	4.7	12.5	36.8	0.457
4	13	4	8	10.8	10.4	18.6	5.9	10.4	0.2	18.8	6.0	10.6	35.4	0.305
2	15	3	7	7.7	7.6	25.2	7.5	11.7	0.0	25.2	7.6	11.7	44.5	0.753
3	14	3	7	9.0	8.6	23.0	10.6	7.0	0.1	23.1	10.7	7.2	41.0	0.510
4	13	3	7	10.8	9.3	24.7	14.0	5.7	2.1	26.8	16.1	7.8	50.6	0.437
3	14	4	7	11.2	10.2	20.2	3.8	13.2	1.0	21.2	4.8	14.2	40.2	0.320
4	13	4	7	13.5	11.1	19.6	5.5	11.2	5.4	25.0	10.9	16.6	52.6	0.291

Smoothed data



21QF Honda Civic LHD Frontal Impact 19/11/2004 15.6m/s

LCW Maxima - Variance and Homogeneity criteria

First Column	Last Column	First row	Last row	Target (max) load kN	Average (max) load kN	Cell Variance	Row Variance	Column Variance	Target Criterion	Cell homogeneity criterion	Row homogeneity criterion	Column homogeneity criterion	Overall homogeneity criterion	Relative homogeneity criterion
2	15	3	8	8.2	7.9	57.1	16.3	23.9	0.1	57.2	16.4	24.0	97.6	1.448
3	14	3	8	9.6	9.1	56.9	21.9	18.2	0.2	57.1	22.1	18.4	97.6	1.064
2	15	4	8	9.9	8.7	63.0	15.9	29.3	1.3	64.3	17.1	30.6	112.0	1.154
3	14	4	8	11.5	10.0	61.7	21.4	22.5	2.2	63.9	23.6	24.7	112.2	0.849
4	13	4	8	13.8	11.5	60.9	30.5	14.5	5.4	66.3	35.9	19.9	122.2	0.642
2	15	3	7	9.9	9.0	61.7	13.4	32.3	0.8	62.5	14.2	33.1	109.8	1.131
3	14	3	7	11.5	10.3	58.8	17.7	24.6	1.4	60.2	19.1	26.0	105.2	0.797
4	13	3	7	13.8	11.8	56.8	25.6	16.3	4.0	60.7	29.6	20.2	110.5	0.581
3	14	4	7	14.4	11.7	61.3	12.0	33.1	6.9	68.2	18.8	40.0	127.1	0.616
4	13	4	7	17.2	13.4	55.5	18.5	22.3	14.4	69.9	32.9	36.7	139.5	0.469

Unsmoothed data

First Column	Last Column	First row	Last row	Target (max) load kN	Average (max) load kN	Cell Variance	Row Variance	Column Variance	Target Criterion	Cell homogeneity criterion	Row homogeneity criterion	Column homogeneity criterion	Overall homogeneity criterion	Relative homogeneity criterion
2	15	3	8	7.6	8.7	36.6	8.7	21.9	1.3	38.0	10.0	23.2	71.2	1.242
3	14	3	8	8.8	10.0	32.1	11.9	14.7	1.4	33.5	13.4	16.2	63.1	0.809
2	15	4	8	9.1	9.8	39.6	5.4	30.3	0.5	40.1	5.9	30.8	76.7	0.929
3	14	4	8	10.6	11.3	32.1	7.3	21.2	0.5	32.5	7.7	21.6	61.9	0.551
4	13	4	8	12.7	12.7	26.8	8.9	14.1	0.0	26.8	8.9	14.1	49.7	0.307
2	15	3	7	9.1	9.3	40.4	9.3	23.9	0.0	40.5	9.3	24.0	73.7	0.893
3	14	3	7	10.6	10.7	35.3	12.9	15.9	0.0	35.4	13.0	15.9	64.2	0.571
4	13	3	7	12.7	11.9	33.9	17.3	10.5	0.6	34.6	17.9	11.1	63.6	0.393
3	14	4	7	13.3	12.5	32.8	3.4	25.5	0.5	33.3	4.0	26.0	63.3	0.360
4	13	4	7	15.9	14.1	26.5	4.6	17.8	3.3	29.9	8.0	21.2	59.0	0.233

Smoothed data

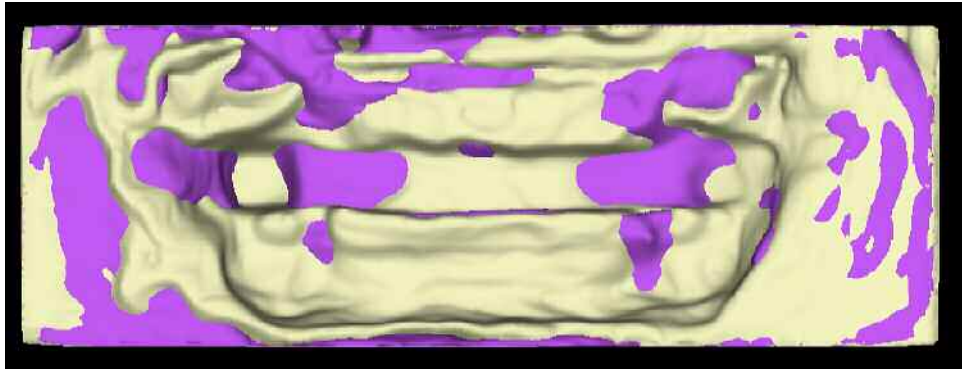


Appendix D: Barrier Deformation Comparison

View showing difference in barrier face deformation (maximum penetration)

Unmodified car – Purple

Modified car – Grey



View showing difference in barrier face deformation (minimum penetration)

Unmodified car – Purple

Modified car – Grey

